Evaluating the Spatial Consequences of a Climate Tipping Point*

José-Luis Cruz
FRB of New York

Klaus Desmet
SMU

Esteban Rossi-Hansberg
University of Chicago

October 7, 2026

Abstract

The Atlantic Meridional Overturning Circulation (AMOC) is a system of ocean currents that plays a key role in regulating global climate, including moderating temperatures in Europe and the North Atlantic. Its potential collapse due to global warming is widely considered one of the more likely climate tipping points. This paper examines the economic implications of such a collapse using a dynamic spatially integrated assessment model (S-IAM) of the world economy. Scandinavia and parts of Russia are predicted to experience significant losses in GDP and welfare, while southern Europe, northern Africa, and Brazil benefit from slightly colder temperatures. S-IAMs generally predict that global warming is especially harmful to low-income regions, but an AMOC collapse could mitigate some of these negative impacts in parts of the developing world while instead harming some of the more advanced economies. This lowers spatial inequality, but global welfare drops by 2.0% by 2200 under an intermediate-emissions scenario.

Keywords: climate tipping points, AMOC, spatially integrated assessment models, geography, development
JEL Codes: F18, F64, O11, Q54, Q56, R11

1 Introduction

A climate tipping point is a critical threshold beyond which the climate system reorganizes, often irreversibly (Lee et al., 2021). One of the most consequential such tipping points is a collapse of the Atlantic Meridional Overturning Circulation (AMOC), a system of ocean currents that transports warm, salty water northward near the surface and returns colder, denser water southward at depth. The AMOC has a profound impact on the global climate, including keeping Western and Northern Europe substantially warmer in winter than other regions at comparable latitudes. Rome, for example, is about 10°C warmer than Chicago in winter despite lying at the same latitude. Global warming weakens these currents, and beyond a critical temperature threshold, the AMOC may begin to collapse.

While climate scientists have studied this tipping point extensively, its economic consequences remain poorly understood. That has not stopped the European media from occasionally describing a potential AMOC shutdown

*Cruz: Federal Reserve Bank of New York, jose-luis.cruz@ny.frb.org, Desmet: Department of Economics and Cox School of Business, Southern Methodist University, Federal Reserve Bank of Dallas, NBER and CEPR, kdesmet@smu.edu, Rossi-Hansberg: Department of Economics, University of Chicago, earossih@uchicago.edu. We thank Julian Tsang for outstanding research assistance, and Elisabeth Vogel for providing historical data and projections for GHG emissions and radiative forcing. Desmet acknowledges support from the National Bank of Belgium through the NBB Research Fellowship Program and from the Dedman College Dean's Research Council at SMU. Rossi-Hansberg thanks the Becker Friedman Institute for Economics and the Spatial Dynamics Incubator for their support. The views expressed herein are those of the author and not necessarily those of the National Bank of Belgium, the Eurosystem, the Federal Reserve Bank of New York, the Federal Reserve Bank of Dallas, or any other person affiliated with the Federal Reserve System.

in apocalyptic terms. The *Daily Express* tabloid, for instance, warned that it would "plunge Europe and [the] UK into [the] ice age" (November 12, 2025), while *The Economist* wrote that a shutdown "could freeze Europe" and suggested that "it could lay waste a continent –specifically, Europe– to an extent that only a nuclear war could outmatch" (August 14, 2025). Without an economic assessment of this climate tipping point, these claims are difficult to evaluate.

This paper quantifies the economic impact of an AMOC collapse across time and space using the spatially integrated assessment model (S-IAM) of Cruz and Rossi-Hansberg (2024). The framework incorporates damage functions for productivity and amenities, and explicitly accounts for spatial linkages through trade, migration and innovation. In response to an AMOC slowdown, trade patterns and migration flows adjust, and innovation adapts endogenously. The model is quantified at a $1^\circ \times 1^\circ$ spatial resolution for the entire globe, enabling projections at a fine geographic scale rather than solely at the regional or country level. Starting in 2022, we simulate the model forward and assume that a tipping point is reached when global mean surface temperature rises to $+3^\circ$C above preindustrial levels (van Westen et al., 2024). Once this threshold is crossed, we impose local temperature changes associated with an AMOC shutdown based on estimates from van Westen and Baatsen (2025), assuming that this temperature shock unfolds gradually over time.

A key finding is that an AMOC collapse may reverse some of the effects of global warming. Relative to a world with global warming but no collapse, the northernmost latitudes, where global warming is most beneficial, experience substantial losses due to significant cooling. Scandinavia, parts of Russia, and Canada see sharp declines in welfare and real GDP. Intermediate and equatorial latitudes, where global warming is most harmful, see the opposite pattern, with Southern Europe, northern Africa, and Brazil experiencing gains in welfare and real GDP per capita. More broadly, the regions suffering the largest welfare losses from global warming tend to benefit most from an AMOC collapse.

This finding becomes even starker when examining the joint effect of global warming with an AMOC shutdown, rather than the isolated contribution of the collapse alone. Under an intermediate-emissions scenario, this joint effect overturns the standard findings of S-IAMs: global warming hurts most regions north of roughly the US-Mexico border and the southern Mediterranean, while much of Africa, Latin America, and Southeast Asia gains. Whereas many S-IAMs predict that global warming increases spatial inequality by disproportionately harming developing regions, our results imply the opposite: some of the advanced economies emerge as the primary losers of global warming, once the collapse of the AMOC is taken into account.

Europe is among the regions most affected if this tipping point is reached. Relative to a world with global warming but no AMOC shutdown, all of northern and northwestern Europe loses welfare under an intermediate-emissions scenario, including the UK, Germany, the Benelux, and parts of France, while only regions close to the Mediterranean benefit. Under a high-emissions scenario, most of Europe gains, with the exception of Scandinavia and Russia. An AMOC collapse thus divides Europe into losers and winners, with the boundary shifting northward as emissions rise: the greater the rise in temperature due to global warming, the more regions benefit from the AMOC-induced cooling.

Despite reversing some of the effects of global warming, an AMOC collapse has an overall negative effect on aggregate welfare under an intermediate-emissions scenario. Relative to a world that experiences global warming but no collapse, aggregate welfare in 2200 declines by 2.0%. The corresponding joint effect of global warming and an AMOC shutdown on aggregate welfare is a drop of 1.3%. This negative impact reflects losses being concentrated in the relatively productive northernmost latitudes. Under a high-emissions scenario, the impact is more benign:

aggregate welfare increases by 1.2%, relative to a world with climate change but no collapse. In this case, global warming does more damage in productive, mid-latitude regions such as Western Europe, so the cooling induced by a collapse does comparatively less harm.

An AMOC shutdown triggers substantial spatial reallocation of population and economic activity. Relative to a baseline with global warming but no such collapse, under an intermediate-emissions scenario population falls by 18.0% in Russia, 25.9% in Scandinavia, 7.2% in the rest of Europe, and 4.1% in North America, while the Middle East, Africa, and Latin America experience modest gains. The impact on real GDP is of similar magnitude, with Russia losing 20.9%, Scandinavia 25.8%, and the rest of Europe 6.3%.

A related way to quantify the importance of spatial mobility is to ask what the impact of an AMOC collapse would be in a counterfactual world where population cannot move in response. Suppressing spatial reallocation magnifies both the regional losses and the regional gains. Consider Scandinavia, where the large negative temperature shock generates substantial outmigration in the full model. Absent migration, density in northern latitudes stays somewhat higher, depressing wages because land is in fixed supply, and further lowering welfare through the negative effect of density on amenities. Higher density does raise innovation and productivity, but not enough to offset these welfare losses. In the aggregate, restricting migration lowers welfare by 2.1% under an intermediate-emissions scenario, relative to an economy where people can respond to an AMOC collapse by moving. As in other S-IAMs, migration is a key adaptation mechanism, so that not allowing people to move magnifies the losses from climate change.

The potential collapse of the AMOC has been studied extensively by climate scientists, with some debate about whether a tipping point is likely to be reached in this century. The most recent report of the Intergovernmental Panel on Climate Change (IPCC) concludes that an AMOC decline is "very likely" over the 21st century, while expressing "medium confidence" that it will not undergo an abrupt collapse before 2100 (Fox-Kemper et al., 2021). In contrast, van Westen et al. (2024) estimate a critical threshold at a global mean surface temperature increase of +3°C above preindustrial levels, concluding an AMOC collapse before the end of the 21st century is more likely than not ($\geq$ 50%) under a middle-of-the-road emissions scenario and very likely ($\geq$ 90%) under a high-emissions scenario. Using a statistical analysis of early warning signals, Ditlevsen and Ditlevsen (2023) estimate a collapse of the AMOC by the middle of this century. Part of the apparent disagreement between the IPCC and these studies may stem from the IPCC referring to an "abrupt" collapse. As shown by Drijfhout et al. (2025), once a tipping point is reached, the shutdown is likely to occur only gradually over the subsequent hundred years. Our approach builds on these findings: we assume that the AMOC starts to weaken once the +3°C threshold is reached, with the transition to its new long-run temperature taking around a century.

Our work also relates to the economics literature on tipping points, which for the most part overlooks the spatially heterogeneous impact of such events. Lemoine and Traeger (2014) and Lontzek et al. (2015) incorporate climate tipping points into a stochastic integrated assessment model to study optimal policy responses, finding that the prospect of future tipping events raises the optimal carbon tax, in some cases substantially. Cai et al. (2016) extend this analysis to five interacting climate tipping points, concluding that the optimal policy requires an immediate and massive reduction in CO_2 emissions.

Within that literature, a small number of studies have evaluated the heterogeneous economic impact of an AMOC collapse across countries. Using an integrated assessment model with country-specific damage functions, Dietz et al. (2021) estimate that an AMOC slowdown reduces the social cost of carbon by 1.4% by reducing damages from warming, particularly in Europe. Anthoff et al. (2016) and Link and Tol (2011) similarly find modest effects,

since the associated cooling largely offsets warming. These models allow for heterogeneity across countries, but do not incorporate spatial linkages in the form of trade and migration. In this sense, they are akin to an accounting exercise in which geographic heterogeneity enters only through country-specific damage functions.

Our paper shows that these spatial linkages matter quantitatively: an AMOC collapse triggers substantial reallocation of population and economic activity across space, and ignoring this margin would overstate the aggregate welfare losses of this climate tipping point. As in other spatial models, migration serves as an adaptation mechanism that mitigates some of the negative impact. Analyzing this tipping point through the lens of a S-IAM is also essential for showing how an AMOC collapse reverses the standard prediction that climate change disproportionately hurts developing regions. Importantly, because an AMOC shutdown is particularly harmful to advanced economies, it overturns the rise in spatial inequality typically associated with climate change.

The rest of the paper is organized as follows. Section 2 provides further details on the AMOC and its possible collapse. Section 3 summarizes the key elements of the S-IAM of Cruz and Rossi-Hansberg (2024) and describes the quantification of an AMOC shutdown. Section 4 discusses the global economic impact of a potential AMOC collapse. Section 5 focuses on the spatial impact of an AMOC collapse. Section 6 concludes.

2 The Collapse of the AMOC as a Climate Tipping Point

The AMOC functions as a conveyor belt driven by thermohaline forces — that is, differences in temperature and salinity. In the subpolar North Atlantic, surface ocean waters lose heat to the cold atmosphere, increasing their density. In addition, waters from the subtropics, made saltier by evaporation, are transported northward. This raises the salinity of surface waters in the North Atlantic, further increasing their density. The resulting density differences between surface and deep waters in the North Atlantic lead to deep convection, the process of waters moving vertically to depths of ∼1,000–4,000 m. To balance the mass of water in the ocean, deep waters must rise in other regions, most notably in the Southern Ocean. This vertical movement, whereby surface waters sink in the North Atlantic and rise back to the surface in the Southern Ocean, is referred to as overturning. It is what gives rise to the conveyor belt nature of the AMOC which transports warm surface water from the subtropics to the North Atlantic and returns cold water at depth (Figure 1).

With global warming, surface waters in the North Atlantic become less cold, and with the melting of the Greenland ice sheet, their salinity declines. Both mechanisms make the surface water less dense, weakening deep convection. As the AMOC slows down, less salty water from the subtropics is transported northward. This makes surface waters in the North Atlantic even lighter, further weakening the overturning. Once a certain threshold is reached, this salt advection feedback mechanism becomes self-reinforcing and a climate tipping point is crossed: the AMOC collapses, as it transitions from a state with strong, deep overturning to one with weak, shallow overturning.

An AMOC shutdown redistributes heat across the globe, cooling large parts of the Northern Hemisphere while warming parts of the Southern Hemisphere. Because it is triggered by global warming, in some regions the cooling from an AMOC collapse may offset the temperature increases due to climate change. In high northern latitudes, such as Scandinavia and Russia, the net effect is expected to be substantial cooling, whereas in certain areas below the Equator, including Argentina, the effects of global warming may be amplified. An AMOC shutdown can therefore be interpreted as a spatial shock, affecting productivity and well-being heterogeneously across locations. As noted above, the temperature response to a tipping point is unlikely to be abrupt; instead, it is expected to unfold gradually over time (Drijfhout et al., 2025). Despite this, the literature commonly refers to this tipping

Figure 1: The Atlantic Meridional Overturning Circulation (AMOC)

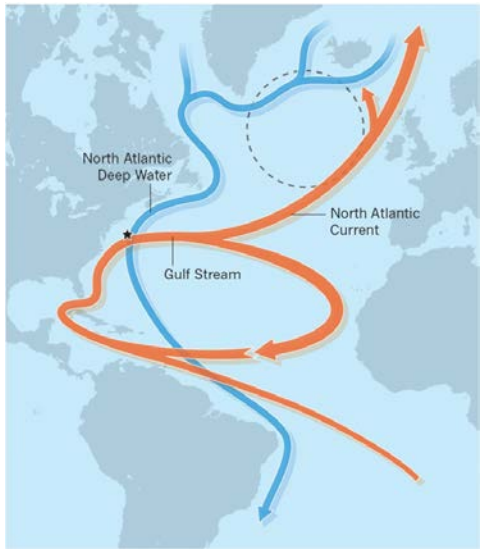

Source: Praetorius (2018). The Atlantic Meridional Overturning Circulation (AMOC) transports warm, salty surface water from the subtropics to the North Atlantic and returns cold water at depth.

point as a "collapse" of the AMOC. Here, we follow this convention, but model its effect on temperature as a gradual transition.

3 Framework and Quantification

To analyze the spatial economic impact of a potential AMOC collapse, we use the S-IAM developed by Cruz and Rossi-Hansberg (2024) and combine it with high-resolution, time-varying estimates of the temperature effects of such a collapse. In this section, we briefly describe the key features of the model and its quantification, and refer the interested reader to the original paper for further details.

3.1 Framework

Figure 2 provides a graphical overview of the Cruz and Rossi-Hansberg (2024) model. Individuals reside in different locations across the globe, where they work and consume. They may also choose to migrate, albeit at a cost. Firms use labor and a combination of clean and dirty energy inputs, invest in innovation, and engage in costly trade. Economic activity, through the use of fossil fuels, generates global warming, which in turn affects firms productivity as well as local consumption amenities.

Endowments and preferences. The world economy occupies a two-dimensional surface S, where each location is defined by a point $r \in S$ with land density $H(r)$. In each period t, the world economy is populated by an exogenous mass L_t of agents.

An agent derives utility from consuming a set of differentiated varieties, $c_t^{\omega}(r)$, from local amenities, $b_t(r)$, and from their idiosyncratic preference for the location where they reside, $\varepsilon_t^i(r)$. When agents move from r to s in period t, their utility is discounted by a permanent flow utility cost $m(r, s)$ incurred in t and all subsequent periods.

Figure 2: Graphical Overview of the S-IAM by Cruz and Rossi-Hansberg (2024)

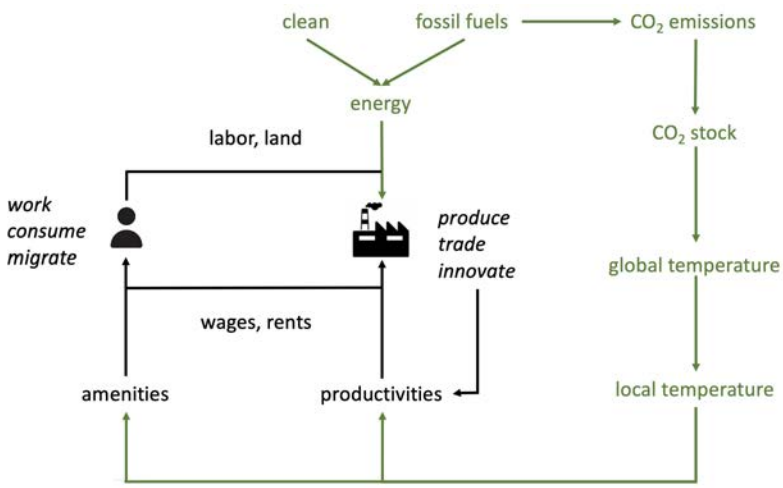

More specifically, the period utility of an agent i residing in location r in period t, having previously resided in locations $\bar{r}_- = (r_0, \ldots, r_{t-1})$, is given by:

$$u_t^i(\bar{r}_-, r) = \underbrace{\left[\int_0^1 c_t^\omega(r)^\rho \mathrm{d}\omega\right]^{1/\rho}}_{\text{consumption}} \underbrace{b_t(r)\varepsilon_t^i(r)}_{\text{amenities}} \underbrace{\prod_{\ell=1}^{t} m(r_{\ell-1}, r_\ell)^{-1}}_{\text{moving costs}},$$

where $\rho/(1-\rho)$ is the elasticity of substitution between the different varieties. Agents receive a wage $w_t(r)$ for work and per-capita land rents $R_t(r)/L_t(r)$, where $L_t(r)$ denotes local population density. Thus, per-capita real income is

$$y_t(r) = \left(w_t(r) + R_t(r)/L_t(r)\right)/P_t(r),$$

with $P_t(r)$ being the ideal CES price index in location r.

Local amenities diminish with density, so

$$b_t(r) = \bar{b}_t(r) L_t(r)^{-\lambda},$$

where $\lambda \geq 0$ determines the degree of congestion, and where the fundamental component of amenities, $\bar{b}_t(r)$, evolves over time as a function of temperature,

$$\bar{b}_t(r) = \Big(1 + \Lambda^b(\Delta T_t(r), T_{t-1}(r))\Big)\bar{b}_{t-1}(r), \tag{1}$$

with $\Lambda^b(\cdot)$ being the amenities damage function. Depending on a location's initial temperature and the magnitude of the temperature change it experiences, amenities may either deteriorate or improve over time. This constitutes the first channel through which climate change affects the economy. In addition, the preference shock $\varepsilon_t^i(r)$ is the realization of a random variable from a Fréchet distribution with shape parameter $1/\Omega$.

The permanent flow utility cost incurred by moving from r to s is the product of an origin-specific cost, $m_1(r)$, and a destination-specific cost, $m_2(s)$. As in Desmet et al. (2018), remaining in the same location is costless, so

$m_2(r) = m_1(r)^{-1}$. Hence, the permanent flow utility cost associated with moving into a location is compensated by a permanent flow utility benefit when moving out of that location. This implies that immigrants in location s only pay the cost associated with moving while residing in s. As a result, the migration decision is fully reversible. This simplifies the forward-looking dynamic migration problem to a sequence of static decisions.

The fraction of households residing in r at period t is given by

$$\frac{L_t(r)H(r)}{L_t} = \frac{u_t(r)^{1/\Omega} m_2(r)^{-1/\Omega}}{\int_S u_t(v)^{1/\Omega} m_2(v)^{-1/\Omega}\,\mathrm{d}v}, \tag{2}$$

where $u_t(r) = b_t(r)y_t(r)$ denotes how individuals value the amenities and the real income of location r. It does not include the idiosyncratic component of utility nor the mobility costs incurred by some individuals to move to r.

Technology. Output per unit of land of a firm in location r producing variety $\omega \in [0,1]$ is given by

$$q_t^\omega(r) = \phi_t^\omega(r)^{\gamma_1} z_t^\omega(r) \left(L_t^\omega(r)^\chi e_t^\omega(r)^{1-\chi}\right)^\mu,$$

where $L_t^\omega(r)$ are labor inputs, $e_t^\omega(r)$ are energy inputs, $\phi_t^\omega(r)$ is productivity due to innovation, and $z_t^\omega(r)$ is an idiosyncratic productivity shifter. Investing in innovation by enhancing productivity requires $\nu\phi_t^\omega(r)^\xi$ units of labor, and the productivity shifter is the realization of a random variable from a Fréchet distribution with c.d.f. $F(z,a) = e^{-a_t(r)z^{-\theta}}$. The scale parameter $a_t(r)$ determines the level of productivity, and it benefits from density,

$$a_t(r) = \bar{a}_t(r)L_t(r)^\alpha,$$

where α determines the strength of agglomeration economies, and where the fundamental level of productivity follows a dynamic process,

$$\bar{a}_t(r) = \Big(1 + \Lambda^a(\Delta T_t(r), T_{t-1}(r))\Big)\phi_{t-1}(r)^{\theta\gamma_1}\left(\int_S D(v,r)\bar{a}_{t-1}(v)\mathrm{d}v\right)^{1-\gamma_2}\bar{a}_{t-1}(r)^{\gamma_2}. \tag{3}$$

Past innovation, $\phi_{t-1}(r)$, raises a location's fundamental productivity, shifting up its distribution of idiosyncratic productivity. Fundamental productivity also depends positively on past technology in its own location, $\bar{a}_{t-1}(r)$, technology diffusion from other locations, $\int_S D(v,r)\bar{a}_{t-1}(v)\mathrm{d}v$, and the productivity damage function, $\Lambda^a(\cdot)$. This is the second channel through which climate change affects the economy. As in Desmet et al. (2018), the model assumes competitive land markets, with firms bidding up land prices until their profits net of innovation costs are zero. Because past innovations are embedded in local productivity, they benefit all potential entrants, so any future gains from current innovations accrue to land, the fixed factor. This simplifies the dynamic forward-looking innovation decision to a sequence of static decisions.

Goods can be traded across locations, at a cost, and trade is balanced location by location. The share of goods consumed at s that are produced in r is then given by a gravity equation,

$$\pi_t(s,r) = \frac{\bar{a}_t(r)L_t(r)^\alpha mc_t(r)^{-\theta}\varsigma(r,s)^{-\theta}}{\int_S \bar{a}_t(v)L_t(v)^\alpha mc_t(v)^{-\theta}\varsigma(v,s)^{-\theta}\,\mathrm{d}v}, \tag{4}$$

where $mc_t(r)$ denotes the marginal cost of production and $\varsigma(r,s)$ represents the iceberg trade cost of shipping a good from r to s.

Energy. Energy is a CES composite of fossil fuels, $e_t^{f,\omega}(r)$, and clean energy, $e_t^{c,\omega}(r)$,

$$e_t^{\omega}(r) = \left(\kappa e_t^{f,\omega}(r)^{\frac{\epsilon-1}{\epsilon}} + (1-\kappa) e_t^{c,\omega}(r)^{\frac{\epsilon-1}{\epsilon}}\right)^{\frac{\epsilon}{\epsilon-1}}.$$

Producing one unit of energy costs $\mathcal{Q}_t^j(r)$ units of labor,

$$\mathcal{Q}_t^f(r) = \frac{f(CumCO2_t)}{\zeta_t^f(r)} \quad \text{and} \quad \mathcal{Q}_t^c(r) = \frac{1}{\zeta_t^c(r)},$$

which depends on $f(\cdot)$, the extraction cost of fossil fuels, and $\zeta_t^j(r)$, the productivity of energy generation. The extraction cost is an increasing and convex function of cumulative carbon extraction, and it tends to infinity as it approaches the total available stock of carbon in the ground. The productivity of energy generation is increasing in the growth of global real GDP per capita, y_t^w:

$$\zeta_t^j(r) = \left(\frac{y_t^w}{y_{t-1}^w}\right)^{\upsilon^j} \zeta_{t-1}^j(r).$$

Relationship between the economy and climate. As discussed above, climate affects the economy through the damage functions for amenities and productivity. Conversely, the economy affects climate through the use of fossil fuels, as CO_2 emissions raise global temperature. Following IPCC (2013), the stock of carbon in the atmosphere, S_t, evolves according to

$$S_{t+1} = S_{\text{pre-ind}} + \sum_{\ell=1}^{\infty}(1-\delta_\ell)\left(E_{t+1-\ell}^f + E_{t+1-\ell}^x\right). \tag{5}$$

where $E_t^f = \int_S \int_0^1 e_t^{f,\omega}(v) H(v)\, \mathrm{d}\omega\, \mathrm{d}v$ denotes the endogenous global CO_2 emissions from fossil fuel combustion, E_t^x denotes exogenous CO_2 emissions from non-fuel sources, $S_{\text{pre-ind}}$ is the preindustrial atmospheric CO_2 stock, and $(1-\delta_\ell)$ is the fraction of CO_2 emissions remaining in the atmosphere ℓ periods later.

Higher atmospheric CO_2 concentrations increase radiative forcing, F_{t+1}, which is given by

$$F_{t+1} = \varphi \log_2(S_{t+1}/S_{\text{pre-ind}}) + F_{t+1}^x, \tag{6}$$

where φ denotes the forcing sensitivity to the atmospheric carbon stock and F_t^x represents radiative forcing from non-CO_2 greenhouse gases.

With positive radiative forcing, when the inflow of energy exceeds the outflow, global temperature increases:

$$T_{t+1} = T_{\text{pre-ind}} + \sum_{\ell=0}^{\infty} \zeta_\ell F_{t+1-\ell}, \tag{7}$$

where $T_{\text{pre-ind}}$ denotes preindustrial global mean surface temperature and ζ_ℓ is the current temperature response to an increase in the radiative forcing ℓ periods earlier. Because our analysis focuses on local temperature changes, we follow Mitchell (2003) and downscale changes in global temperature to the local level by assuming

$$\Delta T_t(r) = g(r) \cdot \Delta T_t \tag{8}$$

where $g(r)$ determines the sensitivity of temperature in cell r to a one °C change in global temperature.

3.2 Quantification and Simulation

The model is quantified following Cruz and Rossi-Hansberg (2024), with two modifications. First, we abstract from explicitly modeling fertility and mortality, taking the time path of aggregate world population, L_t, directly from that paper. Second, we use 2022, rather than 2000, as the base year. This requires updating several data inputs: in particular, high-resolution income data for 2022 come from the newly developed dataset of Rossi-Hansberg and Zhang (2026). Appendix A provides further details on the data used in the quantification.

We simulate the model forward from 2022 until 2200 under two emissions scenarios: a moderate-emissions scenario akin to RCP4.5 and a high-emissions scenario akin to RCP8.5. Specifically, we set the total stock of extractable carbon equal to the cumulative global carbon emissions projected over the next 500 years under RCP4.5 and RCP8.5. Because extraction costs depend on cumulative extraction relative to the total available stock of carbon, emissions from fossil fuels endogenously differ across scenarios. Hence, we do not take the path of fossil fuel emissions directly from the RCP4.5 and RCP8.5 scenarios; instead, it is the economic model, together with the available stock of carbon, that endogenously generates carbon emissions.[1] Despite this caveat, we will continue to refer to these scenarios by their RCP number throughout the rest of the paper. Note also that although recent emissions trends and the falling cost of renewables have made the high-emissions scenario increasingly implausible (Van Vuuren et al., 2026), we retain it as a point of comparison because it helps interpret our results.

Within this framework, we assess the local and global economic consequences of a potential collapse of the AMOC. Based on an analysis of 24 CMIP6 models, van Westen et al. (2024) conclude that a tipping point is likely to be reached when the global mean surface temperature increases by approximately +3°C above preindustrial levels. van Westen and Baatsen (2025) provide high-resolution estimates of the long-run temperature impact. Importantly, once the tipping point is crossed, the transition to this new long-run climate state is expected to be slow and gradual.

Incorporating these insights, we modify the equation governing the evolution of local temperature (8) to account for temperature changes in post-tipping point periods:

$$\Delta T_t(r) = \begin{cases} g(r) \cdot \Delta T_t, & \text{if } t < t_{\text{AMOC}}, \\ g(r) \cdot \Delta T_t + \left(1 - e^{-\phi(t - t_{\text{AMOC}})}\right) \cdot \Delta T_{\text{AMOC}}(r), & \text{if } t \geq t_{\text{AMOC}}. \end{cases} \tag{9}$$

Here, t_{AMOC} denotes the period in which the tipping point of +3°C is reached, $\Delta T_{\text{AMOC}}(r)$ is the total long-run local temperature change associated with an AMOC collapse, and ϕ is a parameter that governs the speed of temperature convergence to the new climate state. We set $\phi = 0.016$, implying that the AMOC loses approximately 80% of its strength within 100 years after the tipping point, consistent with estimates in van Westen et al. (2024).

Figure 3 depicts the long-run winter temperature response to an AMOC collapse under emissions scenario RCP4.5, based on estimates from van Westen and Baatsen (2025). Winter is defined as December-January-February in the Northern Hemisphere and June-July-August in the Southern Hemisphere. We focus on this season because the productivity and amenities damage functions in Cruz and Rossi-Hansberg (2024) are for the winter months.

[1] Emissions from non-fossil combustion and the forcing from non-CO_2 greenhouse gases are taken as exogenous inputs from the RCP scenarios.

Figure 3: Temperature Impact of Full Collapse of AMOC under RCP4.5

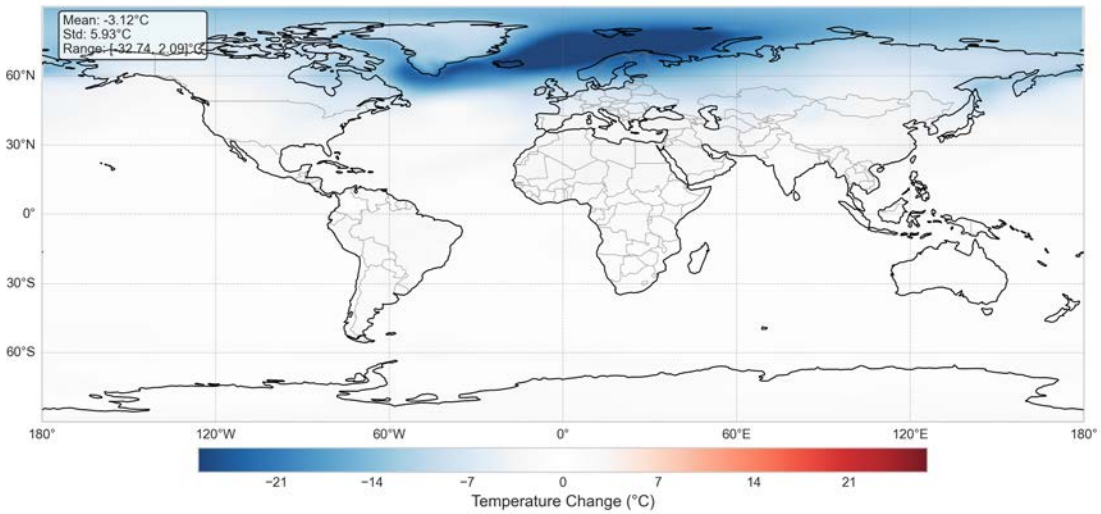

(a) Temperature impact on a scale from -25° to +25°C

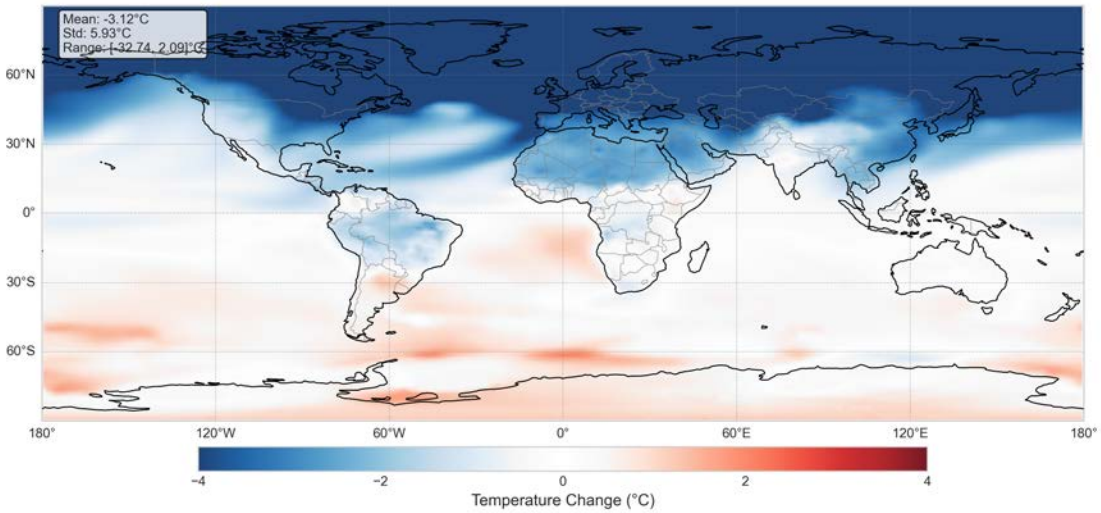

(b) Temperature impact on a scale from -4° to +4°C

This figure shows the difference in average winter temperature (December-January-February) between a full AMOC collapse under RCP4.5 and no such collapse. Panel (b) reproduces panel (a) but restricts the temperature range to -4° to +4°C to make smaller changes visible. Source: van Westen and Baatsen (2025).

The top panel shows pronounced temperature declines concentrated in the high northern latitudes. Around Svalbard, temperatures fall by more than 25°C, while changes elsewhere appear comparatively muted. However, the wide range of temperature changes, from −32.7°C to +2.1°C, masks many other regional impacts. These become clearer in the bottom panel, where the range of temperature changes has been restricted. Most of the Northern Hemisphere, including northern Africa, the Sahara, and Southeast Asia, experiences cooling, whereas parts of the Southern Hemisphere, notably Argentina and Antarctica, show slight warming. Although an AMOC

shutdown is mostly about redistributing heat across the globe, there is a 3.1°C decline in the average temperature across all land and ocean cells.

4 The Spatial Economic Impact of an AMOC Collapse

This section evaluates the economic impact of an AMOC collapse across the globe. As a benchmark, we first simulate our model for a world with global warming, but without an AMOC shutdown. We find the standard result of many S-IAMs: climate change tends to be particularly detrimental for less developed regions close to the Equator, while advanced economies are less impacted and the northernmost latitudes even gain.

To examine the economic consequences of the AMOC shutting down, we then consider two comparisons. First, we compare an AMOC collapse to a baseline with global warming but no such collapse. We find that the shutdown tends to mitigate the adverse effects of climate change in regions that would otherwise be harmed, while it negatively affects some advanced northern economies that would not suffer losses from global warming in the absence of an AMOC tipping point. Second, we compare the overall impact of climate change, including an AMOC collapse, to a world without further warming. Depending on the emissions scenario, the geography of which regions lose or gain is different.

4.1 Benchmark: Global Warming Without an AMOC Collapse

Figure 4 depicts the welfare impact of global warming in 2100 and 2200, assuming the AMOC does not collapse. Specifically, it shows the ratio of welfare under either a high- or an intermediate-emissions world to welfare in a counterfactual world without anthropogenic CO_2 emissions after 2022. The reference point is thus not a world at preindustrial temperatures that never experienced global warming, but rather a world with no further climate change beyond 2022.

Global warming adversely affects most regions of the world, with the exception of those roughly north of the 50th latitude, such as Scandinavia, Russia, and Canada. The richest economies sit at the cusp, gaining or losing little. As expected, while the results are qualitatively similar, the spatial effects are smaller under the intermediate-emissions scenario (RCP4.5), shown in the bottom panels, than under the high-emissions scenario (RCP8.5), shown in the top panels. Recall that under RCP4.5 emissions peak in the mid-21st century and then start to decline, leaving the average global temperature in 2200 close to its 2022 level.[2] At the aggregate level, continued global warming generates by 2200 a modest welfare gain of 0.7% under RCP4.5 and a sizable loss of 6.4% under RCP8.5.[3] The fact that by 2022 global temperatures were already ~ 1.5°C above preindustrial levels explains the relatively minor impact of further global warming under RCP4.5; had the comparison instead been with temperatures in 2000 or in preindustrial times, that scenario would show a welfare loss as well.

[2]To make this limited effect more visible, Appendix Figure B.1 reproduces panels (c) and (d) but restricts the range of the welfare ratio from 0.95 to 1.05.

[3]Global warming incentivizes some people to engage in costly migration. In equilibrium, net of the migration cost, movers have the same ex-ante utility as stayers. To compute the population-weighted aggregate welfare in a world with warming, we therefore use the original distribution of population from a world without warming as weights. This aggregate welfare measure adequately accounts for the moving costs incurred.

Figure 4: Benchmark: Welfare Impact of Global Warming Without an AMOC Collapse

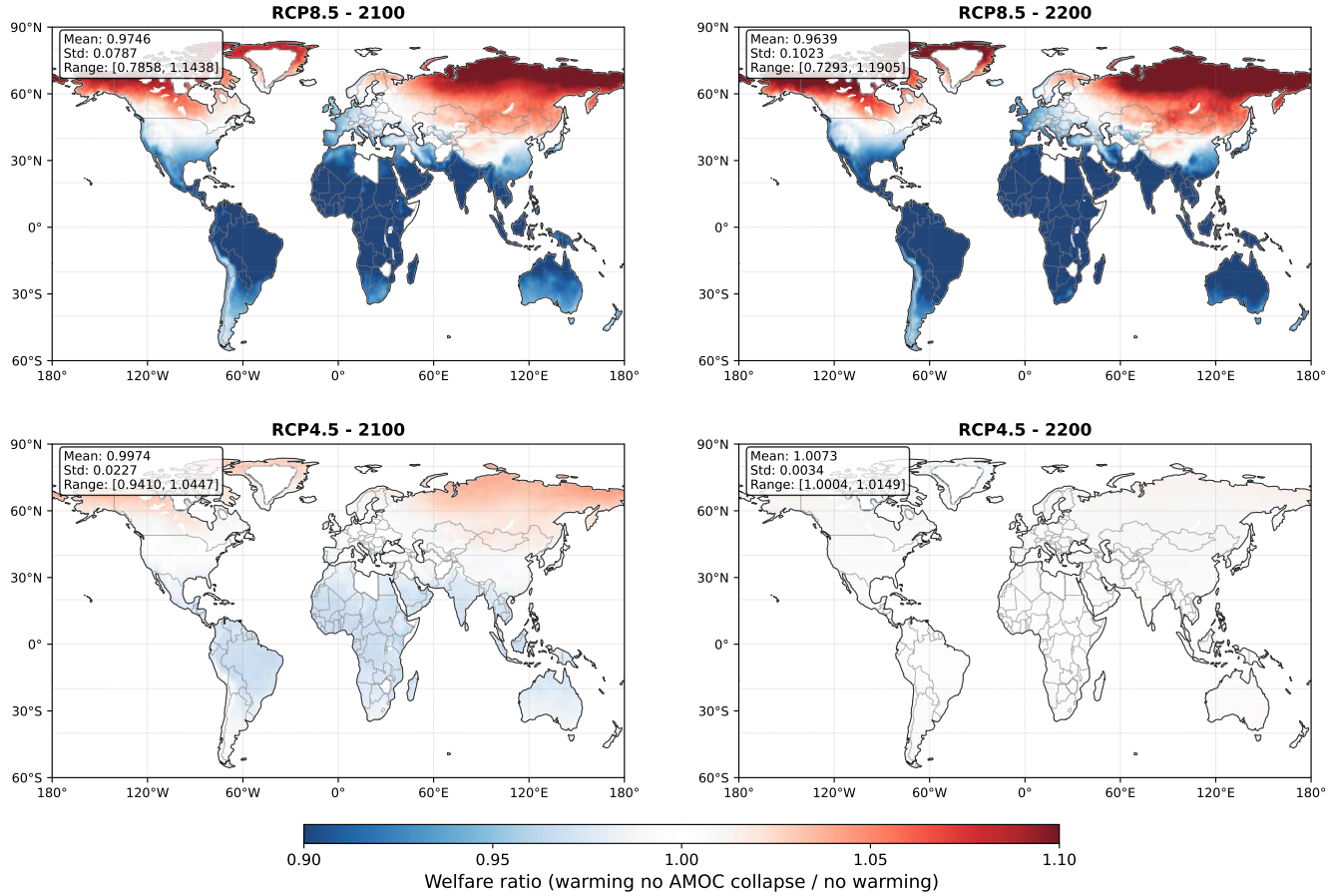

This figure shows welfare in a world with global warming and no AMOC collapse relative to welfare in a world without further global warming post 2022, for RCP8.5 in 2100 (panel (a)) and 2200 (panel (b)), and for RCP4.5 in 2100 (panel (c)) and 2200 (panel (d)). The mean reported in the top left corner of each map is the unweighted average across grid cells.

4.2 First Comparison: Global Warming With and Without an AMOC Collapse

As a first comparison, we examine the welfare impact of an AMOC collapse relative to a world with global warming but no AMOC shutdown. As previously shown in Figure 3, an AMOC collapse leads to a dramatic cooling in the northernmost latitudes of Europe. More broadly, most of the Northern Hemisphere experiences lower temperatures, including northern Africa, Brazil, and Southeast Asia. In contrast, temperatures increase modestly in the Southern Hemisphere, most notably in parts of Argentina.

These temperature changes suggest that an AMOC collapse may reverse some of the spatial economic effects of global warming. In the Northern Hemisphere, we would expect the highest latitudes, where global warming is beneficial, to experience substantial welfare losses due to sharp cooling. In contrast, we would expect intermediate and more equatorial latitudes, where global warming is harmful, to see improved outcomes. This pattern is borne out in Figure 5, which reports the ratio of welfare under an AMOC collapse to welfare under a baseline with global warming but no collapse. Canada, Russia, and Scandinavia experience welfare losses, whereas northern Africa,

Figure 5: First Comparison: Welfare With an AMOC Collapse vs. Welfare Without an AMOC Collapse

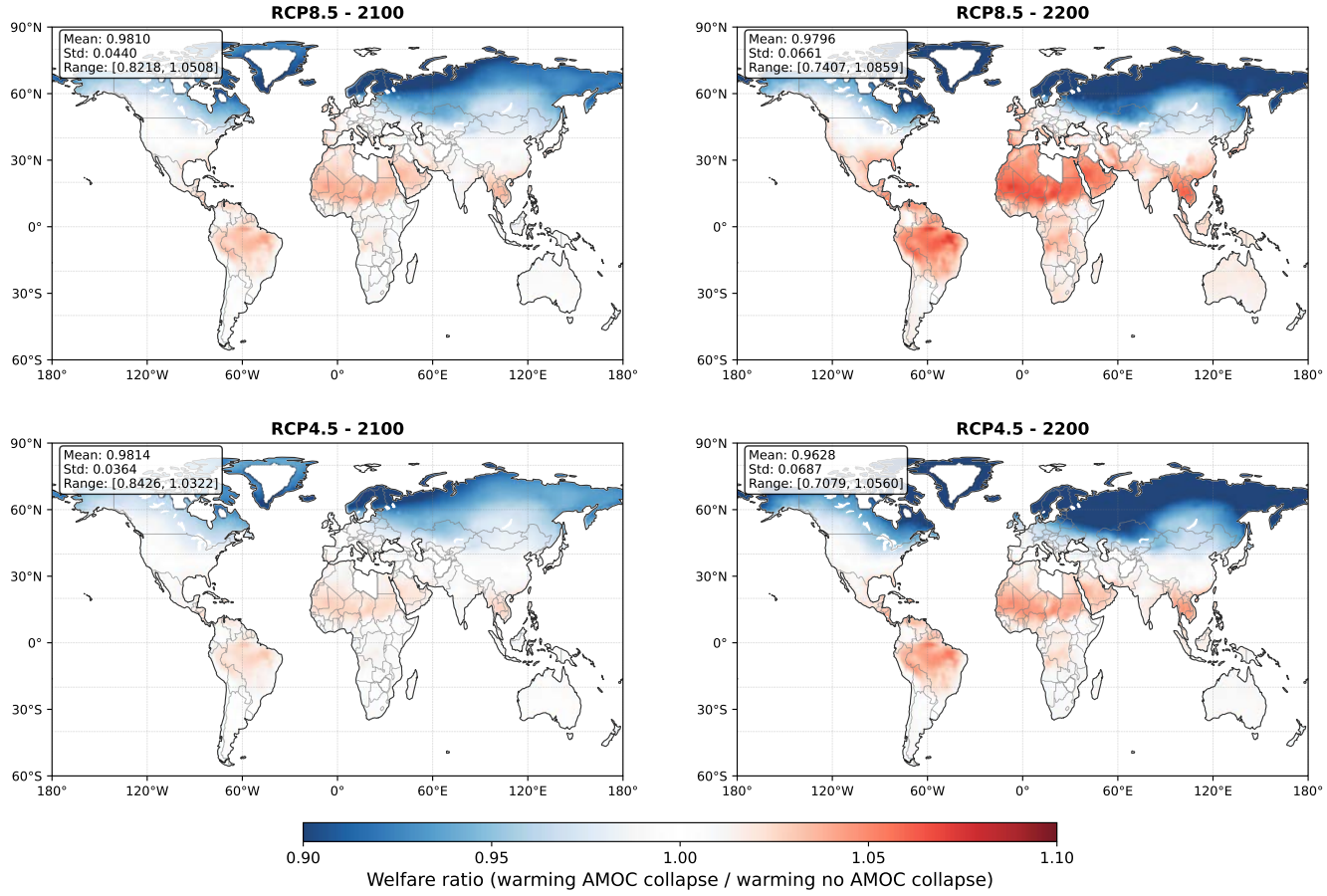

This figure shows welfare in a world with global warming and an AMOC collapse relative to a world with global warming but without an AMOC collapse, for RCP8.5 in 2100 (panel (a)) and 2200 (panel (b)), and for RCP4.5 in 2100 (panel (c)) and 2200 (panel (d)). The mean reported in the top left corner of each map is the unweighted average across grid cells.

Brazil, and Southeast Asia experience welfare gains. The qualitative patterns are similar under RCP8.5 (top panel) and RCP4.5 (bottom panel), though gains in intermediate latitudes are larger under the high-emissions scenario. This result is intuitive: because welfare losses in these regions are convex in the degree of global warming, the temperature reductions associated with an AMOC shutdown generate disproportionately larger benefits.

Figure 6 provides an alternative way of showing that regions suffering the largest welfare losses from global warming tend to benefit most from an AMOC collapse. For the year 2200 and RCP4.5, it plots the welfare impact of a collapse (relative to a global warming baseline without a collapse) against the welfare impact of global warming (relative to a scenario without further global warming). The left panel includes all grid cells of the world, whereas the right panel focuses on Europe and Russia. The negative relationship indicates that locations experiencing smaller losses (or larger gains) from global warming tend to gain less (or lose more) from an AMOC shutdown.

To further examine the losses and gains from an AMOC collapse, Figure 7 shows the distribution of welfare changes across grid cells. Several findings stand out. First, although an AMOC collapse reverses some of the

Figure 6: Welfare Impact of an AMOC Collapse and Losses from Climate Change (RCP4.5 in 2200)

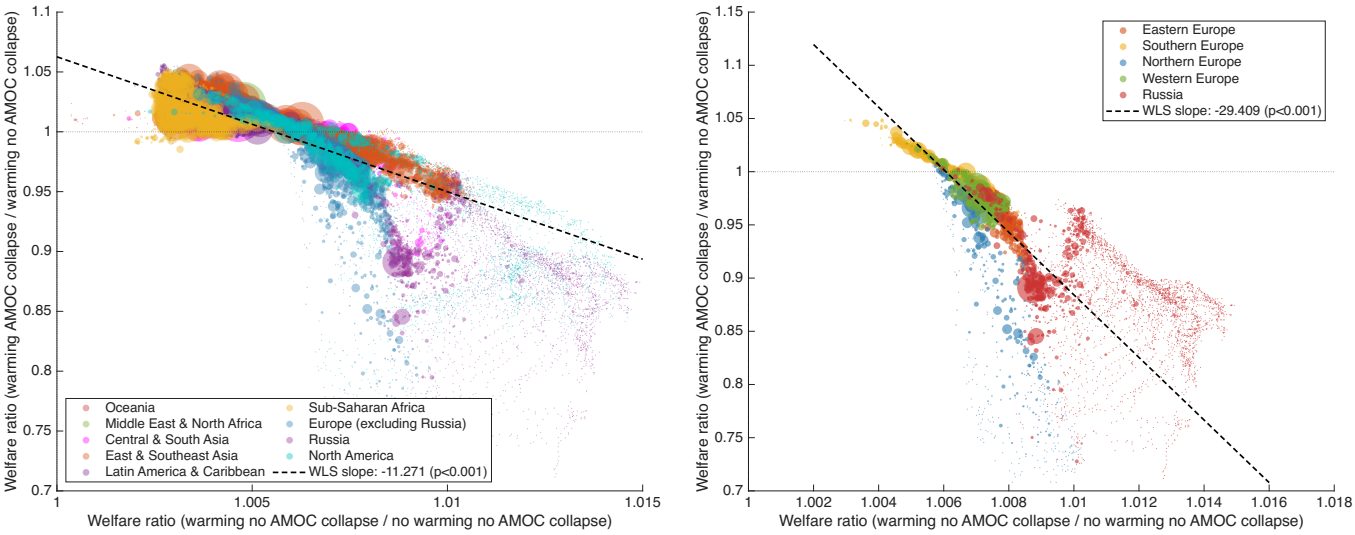

(a) World (b) Europe and Russia

For the year 2200 and RCP4.5, this figure shows a scatter plot of the percentage change in welfare induced by an AMOC collapse (relative to a world with global warming but no collapse) against the percentage change in welfare induced by global warming (relative to a world with no further global warming post 2022). Panel (a) shows all grid cells of the world, whereas panel (b) only shows Europe. Each dot represents a grid cell, with the size proportional to population in 2022 and the color representing the region.

Figure 7: Distribution of Welfare Losses and Gains from the Collapse of the AMOC

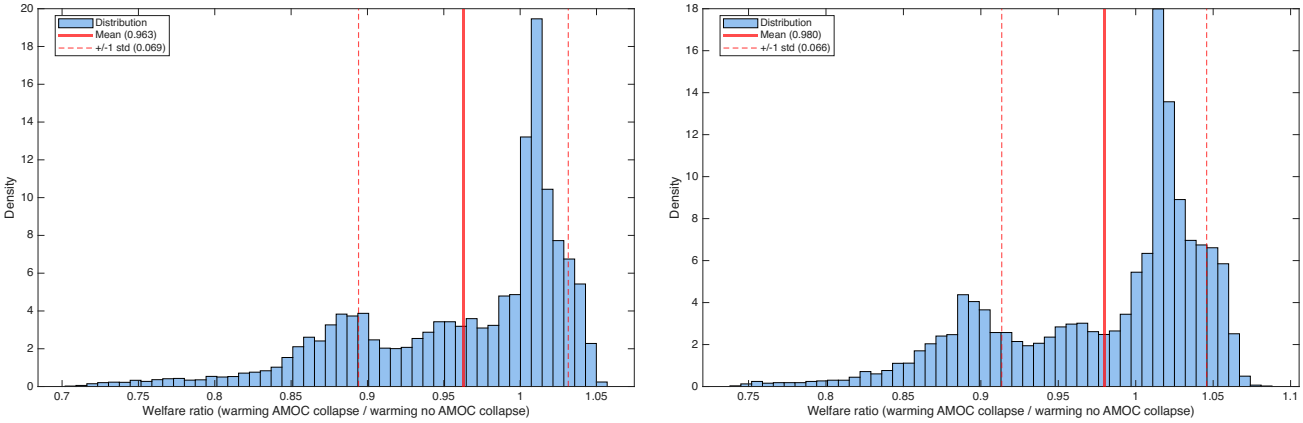

(a) Welfare ratio (RCP4.5 in 2200) (b) Welfare ratio (RCP8.5 in 2200)

This figure plots the distribution of welfare changes induced by an AMOC collapse in 2200, relative to a world with global warming but no collapse. The left panel is for RCP4.5, and the right panel for RCP8.5. The vertical lines in each figure represent the unweighted average and standard deviation across grid cells.

welfare effects of global warming, the average grid cell experiences a welfare loss of 3.7% under RCP4.5. Second, because global warming is more damaging under RCP8.5, the cooling induced by an AMOC collapse is beneficial in a larger number of grid cells, resulting in a smaller average welfare loss. Third, the distribution of welfare changes is asymmetric. Gains are modest and concentrated in the range of 1–5%, whereas losses exhibit a long left

tail, with some locations losing more than 20%. These large losses are concentrated in the northernmost latitudes, where cooling is most severe.

Turning to aggregate effects, Figure 8 compares the time path of aggregate welfare under an AMOC collapse with that of the baseline without collapse. In 2200, an AMOC shutdown generates a projected aggregate welfare loss of 2.0% under RCP4.5, but a modest gain of 1.2% under RCP8.5. As discussed above, cooling in the northern latitudes is less detrimental in the high-emissions scenario, since global warming is more severe absent a collapse.

Figure 8: Aggregate Welfare Effect of a Collapse of the AMOC

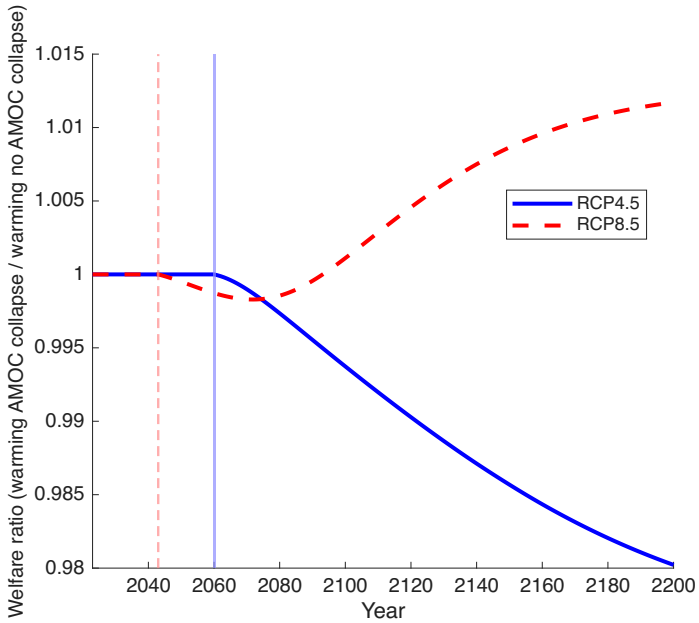

This figure shows the population-weighted aggregate welfare change induced by an AMOC collapse, relative to a world with global warming but no collapse, for the period 2022–2200. The solid curve is for RCP4.5, and the dashed curve for RCP8.5. The corresponding vertical lines indicate when the tipping point is reached.

4.3 A Tale of Two Europes

We now turn to the effect of a weakening AMOC on the different regions of Europe, the continent expected to be most affected by this climate tipping point. Given the sometimes apocalyptic statements in the European media, it is useful to take a closer look at what our model predicts for this part of the world.

Figure 9 shows the welfare impact in 2200 of an AMOC collapse relative to a world with global warming but no AMOC shutdown. It is a close-up of the two right panels in Figure 5. Under the more extreme RCP8.5, with the exception of Scandinavia and Russia, most of Europe experiences a welfare gain from an AMOC collapse. Under RCP4.5, the boundary between losers and winners shifts southward. In this intermediate-emissions scenario, all of northern and northwestern Europe loses, including the UK, Germany, the Benelux and parts of France, while only regions close to the Mediterranean benefit. An AMOC collapse thus splits Europe into losers and winners, with the location of the boundary between the two depending on the emissions scenario. Given that welfare losses from global warming tend to be convex in temperature, the cooling from an AMOC collapse is more beneficial to more regions under the high-emissions scenario.

Figure 9: Welfare Impact on Europe of an AMOC Collapse

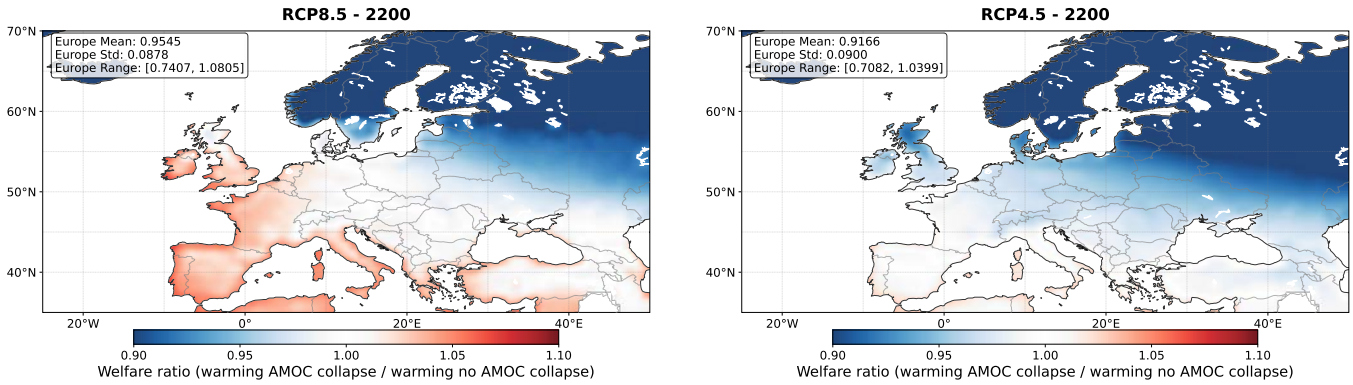

This figure shows welfare in an economy with global warming and an AMOC collapse relative to welfare in an economy with global warming but without an AMOC collapse, in 2200 for RCP8.5 (left panel) and RCP4.5 (right panel). The mean reported in the top left corner of each map is the unweighted average across grid cells.

An AMOC collapse lowers aggregate welfare in Europe by 3.5% under RCP4.5, a larger loss than the 2.0% for the world as a whole. Under RCP8.5, in contrast, Europe experiences a modest welfare gain of 0.8%, slightly smaller than the 1.2% gain globally. This small positive effect reflects the benefits of cooling in southern Europe and the resulting population shift toward those regions.

Figure 10: Effect of an AMOC Collapse on Productivity and Amenities in Europe

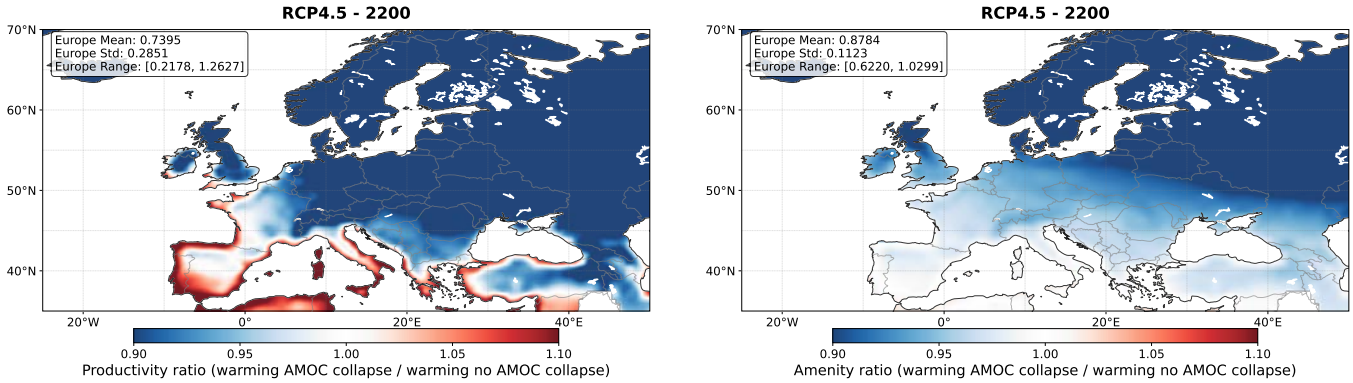

(a) Productivity ratio (b) Amenities ratio

Panel (a) of this figure shows the productivity ratio in an economy with global warming and an AMOC collapse relative to an economy with global warming but without an AMOC collapse, in 2200 for RCP4.5. Panel (b) shows the corresponding amenities ratio. The mean reported in the top left corner of each map is the unweighted average across grid cells.

To unpack the welfare effect of an AMOC collapse on the different regions of Europe, we decompose the associated temperature shock into its effects on productivity and amenities. As shown in panel (a) of Figure 10, under RCP4.5 a collapse of the AMOC improves productivity in southern Europe and some of the coastal regions. In contrast, when looking at the effect on amenities in panel (b), the boundary between losers and winners shifts

southward, with much of Europe experiencing worse amenities.

This divergence reflects subtle differences in the damage functions of productivity and amenities. The average winter temperature that maximizes productivity (1.6°C) is lower than the one that maximizes amenities (8.6°C). As a result, cooling induced by an AMOC collapse may, in some regions, improve productivity while simultaneously reducing amenities. Western Europe falls within the temperature range where these two effects pull in opposite directions.

4.4 Second Comparison: AMOC Collapse Relative to No Further Warming

As a second comparison, we examine the welfare impact of an AMOC collapse relative to a world without further global warming. Whereas the previous subsection compared global warming with and without an AMOC collapse, here we assess the overall impact of climate change under the assumption that an AMOC collapse occurs once the global mean temperature exceeds the +3°C threshold. This second comparison thus captures the joint impact of the previous two exercises: continued global warming augmented by the collapse of the AMOC relative to an economy where temperatures stop changing after 2022.

Figure 11 depicts the ratio of welfare in a world with an AMOC collapse relative to a counterfactual world with no further global warming, for the years 2100 and 2200, under both RCP8.5 (top panels) and RCP4.5 (bottom panels). This comparison thus represents our estimate of the overall effect of climate change once the possibility of an AMOC collapse is taken into account.

Comparing the top panels of Figures 11 and 4 yields two key findings. First, under the more extreme high-emissions scenario RCP8.5, fewer regions benefit from further global warming once the possibility of an AMOC collapse is taken into account. When an AMOC shutdown is ignored, the northernmost latitudes tend to gain from global warming. When instead allowing for a shutdown, the extreme cooling in the North Atlantic offsets these gains, so that Scandinavia and parts of Russia and Canada lose from global warming beyond 2022, and only the region around Alaska continues to benefit.

Second, under the intermediate-emissions scenario RCP4.5, a collapse of the AMOC overturns some of the standard findings of spatially integrated assessment models (S-IAMs). As shown in the bottom-right panel of Figure 11, global warming hurts most regions north of roughly the US-Mexico border and the southern Mediterranean, while much of Africa, Latin America and Southeast Asia gain. Recall that when ignoring an AMOC shutdown, the welfare impact of continued global warming in 2200 under RCP4.5 is minimal, reflecting the small temperature changes relative to 2022. More generally though, many standard evaluations find that the gains and losses from global warming are distributed in a way that increases spatial inequality by disproportionately harming developing regions (Desmet and Rossi-Hansberg, 2015; Carleton and Hsiang, 2016; Conte et al., 2021; Cruz and Rossi-Hansberg, 2024; Carleton et al., 2026). Our results imply the opposite: once we take into account the collapse of the AMOC, advanced economies emerge as the big losers from global warming!

In the aggregate, an AMOC collapse induces a welfare drop of 1.3% under RCP4.5 in 2200, relative to a world without continued global warming. The corresponding number for RCP8.5 is a 5.2% welfare loss. Recall that global warming alone, absent an AMOC collapse, raises welfare by 0.7% under RCP4.5 but lowers it by 6.4% under RCP8.5. Factoring in the possibility of this tipping point therefore turns a modest gain into a loss under RCP4.5 and mitigates the loss under RCP8.5. As noted above, this is because the cooling induced by an AMOC collapse is more beneficial for more regions under the high-emissions scenario.

Figure 11: Welfare Impact of Global Warming With an AMOC Collapse

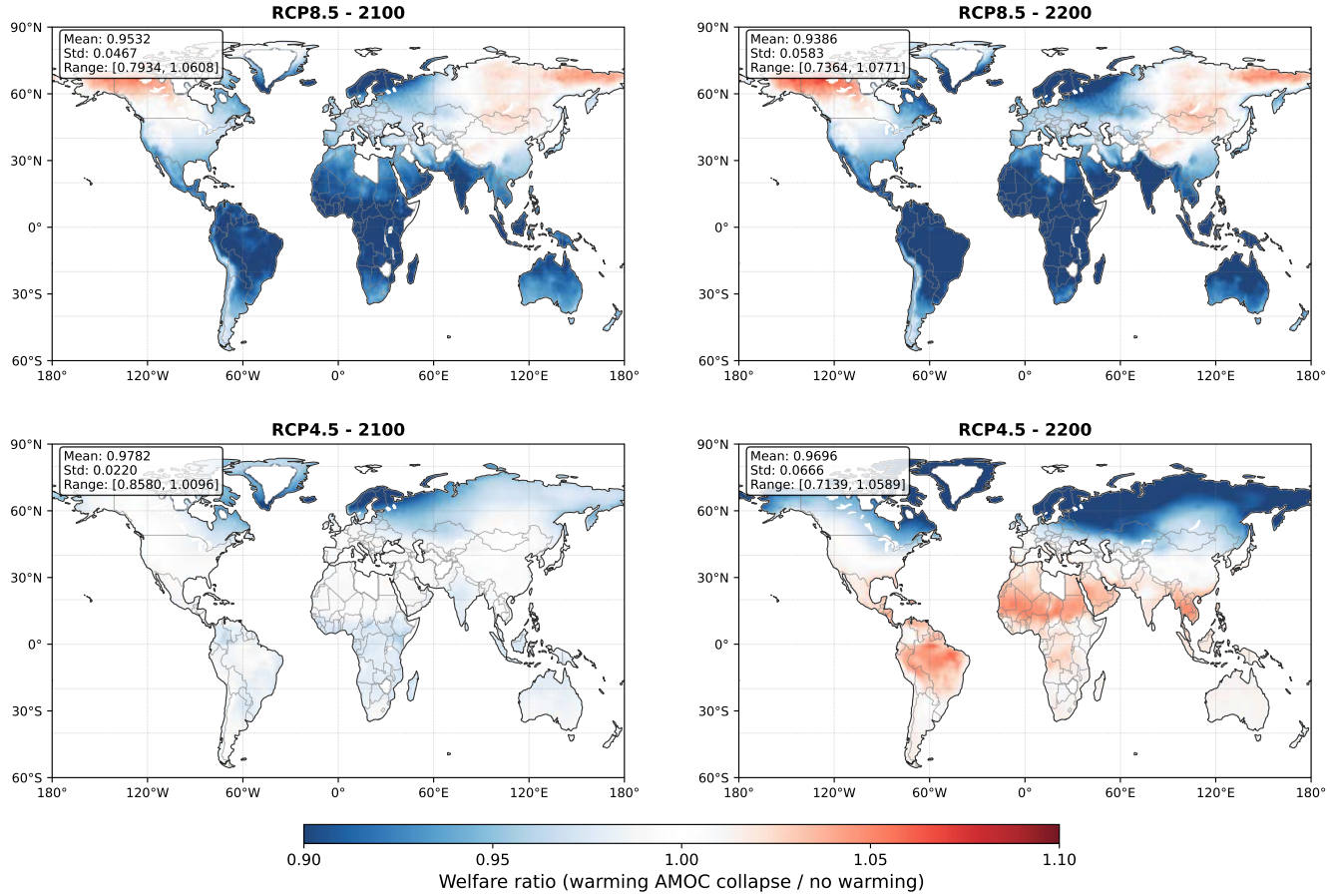

This figure shows welfare in a world with global warming and an AMOC collapse relative to a world without further global warming after 2022. The relative welfare is shown for RCP8.5 in 2100 (panel (a)) and 2200 (panel (b)), and for RCP4.5 in 2100 (panel (c)) and 2200 (panel (d)). The mean reported in the top left corner of each map is the unweighted average across grid cells.

5 The Importance of Space

Previous studies on the economic impact of climate tipping points do not incorporate spatial linkages (Anthoff et al., 2016; Dietz et al., 2021). Relying on country-specific damage functions, these studies evaluate the country-level output impact of temperature changes induced by a climate tipping point, abstracting from the possibility that individuals may migrate in response to productivity or amenities changes and from how such population reallocation affects trade and innovation. To analyze the quantitative importance of spatial reallocation in our S-IAM, this section takes two approaches: first, we quantify how population and GDP reallocate across space following an AMOC collapse; second, we quantify how the impact on GDP and welfare would differ if people were unable to reallocate across space.

5.1 Spatial Reallocation of Population and GDP Induced by an AMOC Collapse

In this subsection, we examine the extent of spatial reallocation induced by a slowdown of the AMOC. Specifically, Table 1 reports percentage changes in population and real GDP by world region in 2200 resulting from an AMOC collapse, relative to a scenario with global warming but no such collapse. Under RCP4.5, Russia experiences a population decline of 17.96%, compared with losses of 25.87% in Scandinavia, 7.17% in the rest of Europe and 4.13% in North America, while the Middle East, Africa, and Latin America register modest gains of approximately 1 to 2%. World population is unchanged by construction. Under RCP8.5, population losses in Europe (excluding Russia and Scandinavia) narrow to 2.68%, as the larger temperature increase associated with this scenario partly offsets the cooling from an AMOC collapse. The regional GDP effects closely mirror these population changes, both qualitatively and quantitatively.

Table 1: Projected Effect of an AMOC Collapse on Population and GDP in 2200

	%Δ Population due to AMOC Collapse		%Δ GDP due to AMOC Collapse	
	RCP4.5	RCP8.5	RCP4.5	RCP8.5
Oceania	-0.79%	-1.66%	-0.70%	-1.23%
Middle East & North Africa	1.66%	2.71%	3.16%	5.82%
Central & South Asia	0.02%	0.07%	0.88%	1.54%
East & Southeast Asia	-1.26%	-0.88%	-0.40%	0.92%
Latin America & Caribbean	1.54%	1.13%	2.11%	2.15%
Sub-Saharan Africa	0.85%	0.38%	1.57%	1.57%
Europe (excluding Scandinavia and Russia)	-7.17%	-2.68%	-6.28%	0.39%
Scandinavia	-25.87%	-18.71%	-25.84%	-16.22%
Russia	-17.96%	-15.48%	-20.93%	-17.01%
North America	-4.13%	-3.08%	-3.63%	-1.73%
Total	0.00%	0.00%	0.39%	1.34%

This table reports the percentage change in population and GDP in 2200 by world region due to an AMOC collapse, relative to a model with global warming but without an AMOC collapse.

5.2 Impact of an AMOC Collapse in the Absence of a Migratory Response

To further assess the importance of spatial linkages, this subsection quantifies the impact of an AMOC collapse on welfare and real GDP absent any migratory response to the shutdown. Specifically, we take the spatial distribution of population in each period from the baseline without an AMOC collapse, and then evaluate the impact of the collapse while holding the distribution of population in each period fixed at this baseline.

Ignoring the migratory response to an AMOC shutdown does not change the qualitative picture of which regions gain and which lose: under RCP4.5, welfare falls in northern latitudes, especially Scandinavia and Russia, and rises in intermediate and equatorial latitudes, particularly in the Northern Hemisphere (Figure 12, panel (a)). In fact, suppressing spatial reallocation amplifies regional losses and gains from an AMOC collapse, relative to a scenario where people can migrate (panel (b)). Focusing on Scandinavia, when people can respond by moving, the

large negative temperature shock triggers significant outmigration, lowering congestion and partially cushioning the welfare loss. Without migration, density in northern latitudes remains higher, depressing wages because land is in fixed supply, and further lowering welfare through the negative effect of density on amenities. Although higher density does raise innovation and productivity, it is not sufficient to offset the welfare loss from congestion. The effect on real GDP per capita is less dramatic, since the channel operating through the congestion of amenities is absent. Even so, northern latitudes continue to see small negative effects relative to the model with migration, as productivity gains are still not large enough to overcome the drop in the marginal product of labor from a rising labor-land ratio (panel (d)). Appendix Figure B.2 reproduces panels (c) and (d) on a more restricted scale for visibility, and Appendix Figure B.3 shows that the same patterns hold under RCP8.5.

Figure 12: Effects of an AMOC Collapse Without Migratory Response (RCP4.5)

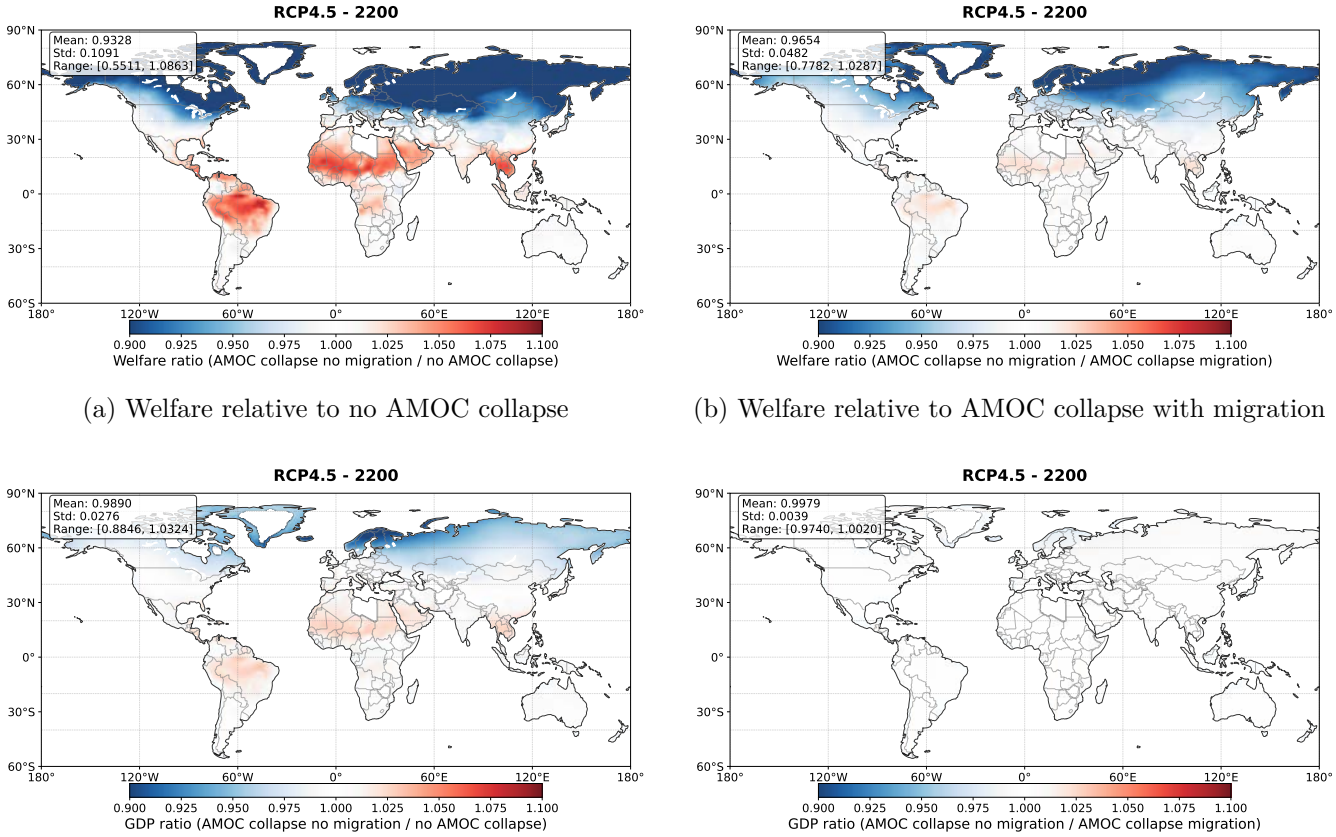

(a) Welfare relative to no AMOC collapse

(b) Welfare relative to AMOC collapse with migration

(c) GDP p.c. relative to no AMOC collapse

(d) GDP p.c. relative to AMOC collapse with migration

Panel (a) shows for the year 2200 and under RCP4.5 the ratio of welfare in an economy with an AMOC collapse but no migratory response to the collapse relative to an economy with no AMOC collapse (panel (a)), and relative to an economy with an AMOC collapse and the possibility to respond to the collapse by migrating (panel (b)). Panels (c) and (d) show the corresponding ratios for real GDP per capita. The mean reported in the top left corner of each map is the unweighted average across grid cells.

Restricting migration lowers welfare by 2.1% by 2200 under RCP4.5, relative to an economy where people can respond to an AMOC collapse by moving (Figure 13, panel (a)). This is consistent with other work showing that migration is an adaptation mechanism, and that restricting movement therefore magnifies the global losses from

climate change (Desmet and Rossi-Hansberg, 2015; Desmet et al., 2021; Cruz, 2023; Conte, 2026). The effect on real GDP per capita is more complex: it is not only smaller, since the congestion of amenities plays no role, but also nonmonotonic, first declining and then recovering. This nonmonotonicity reflects different competing forces. Although more advanced regions, such as Scandinavia, lose from restricting migration, keeping more people in richer regions produces a positive composition effect. Concentrating population in more developed areas also stimulates local innovation, an effect that strengthens over time. Together, these forces explain why the initial effect on global real GDP is negative but eventually turns positive.

Figure 13: Aggregate Effects of an AMOC Collapse Without Migratory Response

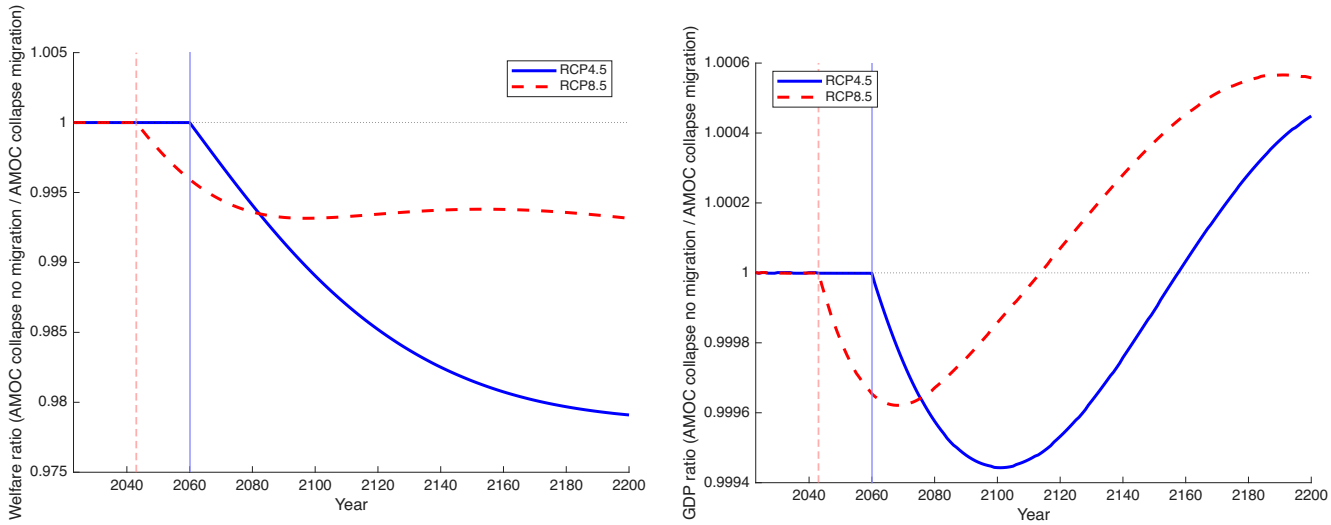

(a) Aggregate welfare relative to AMOC collapse with migration

(b) Aggregate real GDP relative to AMOC collapse with migration

Panel (a) shows the ratio of population-weighted aggregate welfare in an economy with an AMOC collapse and no migratory response relative to an economy with an AMOC collapse and the possibility to migrate. Panel (b) shows the corresponding ratio of aggregate real GDP per capita. The solid curve is for RCP4.5, and the dashed curve for RCP8.5. The corresponding vertical lines indicate when the tipping point is reached.

6 Concluding Remarks

This paper has evaluated the spatial economic impact of a potential collapse of the Atlantic Meridional Overturning Circulation (AMOC), using a spatially integrated assessment model (S-IAM) that allows for costly adaptation through trade, migration and innovation. We find that this tipping point partly overturns the standard finding that global warming increases spatial inequality, as developing regions typically bear the brunt of the economic cost of climate change. However, because an AMOC shutdown is predicted to induce severe cooling in the northernmost latitudes, alongside more modest cooling across much of the Northern Hemisphere, many developing regions in northern Africa, parts of Latin America, and Southeast Asia are projected to gain if such a collapse occurs. In the aggregate, an AMOC collapse leads to a welfare loss of 2.0% under RCP4.5, relative to a global warming scenario that ignores this tipping point. Migratory responses to an AMOC collapse are important: under RCP4.5, Scandinavia loses 25.9% of its population by the year 2200. If we were to shut down migration altogether, global welfare losses would increase by an additional 2.1%.

References

Anthoff, D., F. Estrada, and R. S. Tol (2016). Shutting Down the Thermohaline Circulation. *American Economic Review 106*(5), 602–606.

Cai, Y., T. M. Lenton, and T. S. Lontzek (2016). Risk of Multiple Interacting Tipping Points Should Encourage Rapid CO_2 Emission Reduction. *Nature Climate Change 6*(5), 520–525.

Carleton, T., M. Greenstone, S. Hsiang, A. Hultgren, R. E. Kopp, K. E. McCusker, I. Nath, J. Rising, and A. Rode (2026). The Local Damages from Global Climate Change. Becker Friedman Institute for Economics Working Paper 2026-86.

Carleton, T. A. and S. M. Hsiang (2016). Social and Economic Impacts of Climate. *Science 353*(6304), aad9837.

Conte, B. (2026). Climate Change and Migration: The Case of Africa. *Journal of the European Economic Association*, jvag035.

Conte, B., K. Desmet, D. K. Nagy, and E. Rossi-Hansberg (2021). Local Sectoral Specialization in a Warming World. *Journal of Economic Geography 21*(4), 493–530.

Cruz, J. L. (2023). Global Warming and Labor Market Reallocation. Princeton University Working Paper.

Cruz, J.-L. and E. Rossi-Hansberg (2024, March). The Economic Geography of Global Warming. *The Review of Economic Studies 91*(2), 899–939. rdad042.

Desmet, K., R. E. Kopp, S. A. Kulp, D. K. Nagy, M. Oppenheimer, E. Rossi-Hansberg, and B. H. Strauss (2021). Evaluating the Economic Cost of Coastal Flooding. *American Economic Journal: Macroeconomics 13*, 444–86.

Desmet, K., D. K. Nagy, and E. Rossi-Hansberg (2018). The Geography of Development. *Journal of Political Economy 126*(3), 903 – 983.

Desmet, K. and E. Rossi-Hansberg (2015). On the Spatial Economic Impact of Global Warming. *Journal of Urban Economics 88*(C), 16–37.

Dietz, S., J. Rising, T. Stoerk, and G. Wagner (2021). Economic Impacts of Tipping Points in the Climate System. *Proceedings of the National Academy of Sciences 118*(34), e2103081118.

Ditlevsen, P. and S. Ditlevsen (2023). Warning of a Forthcoming Collapse of the Atlantic Meridional Overturning Circulation. *Nature Communications 14*(1), 1–12.

Drijfhout, S., J. R. Angevaare, J. Mecking, R. M. van Westen, and S. Rahmstorf (2025). Shutdown of Northern Atlantic Overturning After 2100 Following Deep Mixing Collapse in CMIP6 Projections. *Environmental Research Letters 20*(9), 094062.

EDGAR (2025). GHG Emissions Database, Version 9.1.

Energy Institute (2024). Statistical Review of World Energy 2024. London.

Fox-Kemper, B., H. Hewitt, G. Xiao, G. Aðalgeirsdóttir, S. Drijfhout, T. Edwards, N. Golledge, M. Hemer, R. Kopp, G. Krinner, A. Mix, D. Notz, S. Nowicki, I. Nurhati, L. Ruiz, J.-B. Sallée, A. Slangen, and Y. Yu (2021). Chapter 9: Ocean, Cryosphere and Sea Level Change. In V. Masson-Delmotte, P. Zhai, A. Pirani, S. Connors, C. Péan, S. Berger, N. Caud, Y. Chen, L. Goldfarb, M. Gomis, M. Huang, K. Leitzell, E. Lonnoy, J. Matthews, T. Maycock, T. Waterfield, Ö. Yelekçi, R. Yu, and B. Zhou (Eds.), *Climate Change 2021: The Physical Science Basis. Contribution of Working Group I to the Sixth Assessment Report of the Intergovernmental Panel on Climate Change*, pp. 1211–1362. Cambridge University Press.

Friedlingstein, P., M. O'Sullivan, M. W. Jones, R. M. Andrew, J. Hauck, P. Landschützer, C. Le Quéré, H. Li, I. T. Luijkx, A. Olsen, G. P. Peters, W. Peters, J. Pongratz, C. Schwingshackl, S. Sitch, J. G. Canadell, P. Ciais, R. B. Jackson, S. R. Alin, A. Arneth, V. Arora, N. R. Bates, M. Becker, N. Bellouin, C. F. Berghoff, H. C. Bittig, L. Bopp, P. Cadule, K. Campbell, M. A. Chamberlain, N. Chandra, F. Chevallier, L. P. Chini, T. Colligan, J. Decayeux, L. M. Djeutchouang, X. Dou, C. Duran Rojas, K. Enyo, W. Evans, A. R. Fay, R. A. Feely, D. J. Ford, A. Foster, T. Gasser, M. Gehlen, T. Gkritzalis, G. Grassi, L. Gregor, N. Gruber, O. Gürses, I. Harris, M. Hefner, J. Heinke, G. C. Hurtt, Y. Iida, T. Ilyina, A. R. Jacobson, A. K. Jain, T. Jarníková, A. Jersild, F. Jiang, Z. Jin, E. Kato, R. F. Keeling, K. Klein Goldewijk, J. Knauer, J. I. Korsbakken, X. Lan, S. K. Lauvset, N. Lefèvre, Z. Liu, J. Liu, L. Ma, S. Maksyutov, G. Marland, N. Mayot, P. C. McGuire, N. Metzl, N. M. Monacci, E. J. Morgan, S.-I. Nakaoka, C. Neill, Y. Niwa, T. Nützel, L. Olivier, T. Ono, P. I. Palmer, D. Pierrot, Z. Qin, L. Resplandy, A. Roobaert, T. M. Rosan, C. Rödenbeck, J. Schwinger, T. L. Smallman, S. M. Smith, R. Sospedra-Alfonso, T. Steinhoff, Q. Sun, A. J. Sutton, R. Séférian, S. Takao, H. Tatebe, H. Tian, B. Tilbrook, O. Torres, E. Tourigny, H. Tsujino, F. Tubiello, G. van der Werf, R. Wanninkhof, X. Wang, D. Yang, X. Yang, Z. Yu, W. Yuan, X. Yue, S. Zaehle, N. Zeng, and J. Zeng (2025). Global carbon budget 2024. *Earth System Science Data 17*(3), 965–1039.

Golosov, M., J. Hassler, P. Krusell, and A. Tsyvinski (2014). Optimal Taxes on Fossil Fuel in General Equilibrium. *Econometrica 82*(1), 41–88.

International Energy Agency (2024). Greenhouse Gas Emissions from Energy: Highlights. Paris.

IPCC (2013). In *Climate Change 2013: The Physical Science Basis: Contribution of Working Group I to the Fifth Assessment Report of the Intergovernmental Panel on Climate Change*. Cambridge, United Kingdom and New York, NY: Cambridge University Press.

Kummu, M., M. Taka, and J. H. Guillaume (2018). Gridded Global Datasets for Gross Domestic Product and Human Development Index over 1990–2015. *Scientific Data 5*(1), 1–15.

Lee, J.-Y., J. Marotzke, G. Bala, L. Cao, S. Corti, J. Dunne, F. Engelbrecht, E. Fischer, J. Fyfe, C. Jones, A. Maycock, J. Mutemi, O. Ndiaye, S. Panickal, and T. Zhou (2021). Future global climate: Scenario-based projections and near-term information. In V. Masson-Delmotte, P. Zhai, A. Pirani, S. Connors, C. Péan, S. Berger, N. Caud, Y. Chen, L. Goldfarb, M. Gomis, M. Huang, K. Leitzell, E. Lonnoy, J. Matthews, T. Maycock, T. Waterfield, O. Yelekçi, R. Yu, and B. Zhou (Eds.), *Climate Change 2021: The Physical Science Basis. Contribution of Working Group I to the Sixth Assessment Report of the Intergovernmental Panel on Climate Change*, pp. 553–672. Cambridge, United Kingdom and New York, NY, USA: Cambridge University Press.

Lemoine, D. and C. Traeger (2014). Watch Your Step: Optimal Policy in a Tipping Climate. *American Economic Journal: Economic Policy 6*(1), 137–166.

Link, P. M. and R. S. J. Tol (2011). Estimation of the Economic Impact of Temperature Changes Induced by a Shutdown of the Thermohaline Circulation: An Application of FUND. *Climatic Change 104*(2), 287–304.

Lontzek, T. S., Y. Cai, K. L. Judd, and T. M. Lenton (2015). Stochastic Integrated Assessment of Climate Tipping Points Indicates the Need for Strict Climate Policy. *Nature Climate Change 5*(5), 441–444.

Meinshausen, M., Z. R. Nicholls, J. Lewis, M. J. Gidden, E. Vogel, M. Freund, U. Beyerle, C. Gessner, A. Nauels, N. Bauer, et al. (2020). The Shared Socio-Economic Pathway (SSP) Greenhouse Gas Concentrations and Their Extensions to 2500. *Geoscientific Model Development 13*(8), 3571–3605.

Mitchell, T. (2003). Pattern Scaling: An Examination of the Accuracy of the Technique for Describing Future Climates. *Climatic Change 60*, 217–242.

Nicholls, Z. R. J., M. Meinshausen, J. Lewis, R. Gieseke, D. Dommenget, K. Dorheim, C.-S. Fan, J. S. Fuglestvedt, T. Gasser, U. Golüke, P. Goodwin, C. Hartin, A. P. Hope, E. Kriegler, N. J. Leach, D. Marchegiani, L. A. McBride, Y. Quilcaille, J. Rogelj, R. J. Salawitch, B. H. Samset, M. Sandstad, A. N. Shiklomanov, R. B. Skeie, C. J. Smith, S. Smith, K. Tanaka, J. Tsutsui, and Z. Xie (2020). Reduced Complexity Model Intercomparison Project Phase 1: Introduction and evaluation of global-mean temperature response. *Geoscientific Model Development 13*(11), 5175–5190.

Oak Ridge National Laboratory (2024). LandScan Global Population Database.

Praetorius, S. K. (2018). North Atlantic Circulation Slows Down. *Nature 556*, 180–181.

Rohde, R. A. and Z. Hausfather (2020). The Berkeley Earth Land/Ocean Temperature Record. *Earth System Science Data 12*(4), 3469–3479.

Rossi-Hansberg, E. and J. Zhang (2026, August). Local GDP Estimates Around the World. *Journal of Urban Economics 154*, 103871.

Smits, J. and I. Permanyer (2019). The Subnational Human Development Database. *Scientific data 6*(1), 1–15.

Van Vuuren, D. P., B. C. O'Neill, C. Tebaldi, B. M. Sanderson, L. P. Chini, P. Friedlingstein, T. Hasegawa, K. Riahi, B. Govindasamy, N. Bauer, V. Eyring, C. M. N. Fall, K. Frieler, M. J. Gidden, L. K. Gohar, A. Högner, A. D. Jones, J. Kikstra, A. King, R. Knutti, E. Kriegler, P. Lawrence, C. Lennard, J. Lowe, C. Mathison, S. Mehmood, Z. Nicholls, L. F. Prado, Q. Zhang, S. K. Rose, A. C. Ruane, M. Sandstad, C.-F. Schleussner, R. Seferian, J. Sillmann, C. Smith, A. A. Sörensson, S. Panickal, K. Tachiiri, N. Vaughan, S. S. Vishwanathan, T. Yokohata, M. Zecchetto, and T. Ziehn (2026). The Scenario Model Intercomparison Project for CMIP7 (ScenarioMIP-CMIP7). *Geoscientific Model Development 19*(7), 2627–2656.

van Westen, R. M. and M. L. J. Baatsen (2025). European Temperature Extremes Under Different AMOC Scenarios in the Community Earth System Model. *Geophysical Research Letters 52*(12), e2025GL114611. e2025GL114611 2025GL114611.

van Westen, R. M., E. Y. P. Vanderborght, M. Kliphuis, and H. A. Dijkstra (2024). Substantial Risk of 21st Century AMOC Tipping Even Under Moderate Climate Change. *arXiv preprint arXiv:2407.19909*.

A Data and Quantification

Cruz and Rossi-Hansberg (2024) quantify their model for the year 2000. Below, we summarize how we update their procedure to quantify the model for the year 2022, and also list additional data sources.

Population and GDP at $1^\circ \times 1^\circ$. Data on population for the years 2022 and 2023 are taken from the LandScan High Resolution Global Population Data Set (Oak Ridge National Laboratory, 2024). For cells with missing data in 2022, we impute the lowest population density across all cells in the world with non-missing data. We impute missing population in 2023 in a similar fashion. We further restrict the ratio of population in 2023 to population in 2022 to be between 0.94 and 1.08.[4]

Gross Domestic Product in 2022 comes from Rossi-Hansberg and Zhang (2026). They apply a random forest algorithm to high-resolution data on population, nighttime lights, land use, emissions and vegetation to predict cell-level output. For the few missing cells, concentrated in polar latitudes in Northern Canada, Greenland, and Siberia, we set output per capita to the minimum level of their respective subnational units.

Human Development Index at $1^\circ \times 1^\circ$. Since the model inversion identifies $\bar{b}_0(r)/u_0(r)$, but is unable to tell $\bar{b}(r)$ apart from $u_0(r)$, we disentangle a location's amenity from its initial utility with an external estimate of $u_0(r)$. As in Cruz and Rossi-Hansberg (2024), we set $u_0(r) = e^{HDI_0(r)/\psi}$, where $HDI_0(r)$ represents the Human Development Index. We use 2022 data from Smits and Permanyer (2019), who provide information for 1,625 subnational units. Missing observations, primarily for Greenland, are obtained from Kummu et al. (2018).[5]

Temperature at $1^\circ \times 1^\circ$. We take the winter temperature for the year 2022 from the Berkeley Earth Surface Temperature (Rohde and Hausfather, 2020). Winter is defined as the average of January in the Northern Hemisphere and July in the Southern Hemisphere.

Temperature impact of an AMOC collapse at $1^\circ \times 1^\circ$. Our estimates of the long-run temperature impact of an AMOC collapse come from van Westen and Baatsen (2025) who report them for RCP4.5. We take the temperature impact under RCP8.5 to be the same as under RCP4.5. We focus on the impact during the winter months, defined as December-February in the Northern Hemisphere and June-August in the Southern Hemisphere.

CO_2 emissions and clean energy at $1^\circ \times 1^\circ$. We construct gridded energy in two steps. First, we collect 2022 country-level data on CO_2 emissions from EDGAR (2025)[6] and 2022 country-level data on clean energy (interpreted as the sum of nuclear, hydroelectricity and renewables) from Energy Institute (2024).[7] Second, we disaggregate energy use across cells within each country using the spatial distribution of energy for buildings from EDGAR (2025).[8]

[4] This keeps world population growth from 2022 to 2023 equal to its value in the data.

[5] Since that dataset is only available through 2015, we extrapolate the series forward to construct values for 2022.

[6] We allocate international aviation and shipping across countries according to International Energy Agency (2024).

[7] Since this dataset provides information for some aggregate regions, we disaggregate them across countries using the spatial distribution of CO_2 emissions.

[8] For cells with zero emissions data, we have adopted the median CO_2 emissions per capita across all cells in the same country with non-missing data.

Global prices for fossil fuels and clean energy. We construct the global price of fossil fuels as the consumption-weighted average price of coal, oil, and natural gas. Following Golosov et al. (2014), we use the price of oil as our measure of the global price of clean energy. Price data are obtained from Energy Institute (2024), and we use averages over the 2021-2023 period to smooth short-run fluctuations.

Fossil fuel and non-fossil fuel CO_2 emissions and non-CO_2 radiative forcing. Historical data on CO_2 emissions are taken from the Global Carbon Budget 2024 (Friedlingstein et al., 2025), historical forcing from the Reduced Complexity Model Intercomparison Project (Nicholls et al., 2020), and the projections for emissions and forcing from Meinshausen et al. (2020). We define the maxCO_2 parameter as the sum of the RCP-specific CO_2 emissions from fossil fuels from 2022 to 2500.

Projections of global population. From 2023 onward, we take the path of global population from Cruz and Rossi-Hansberg (2024) for each RCP scenario, which we treat as exogenously given in our simulations for RCP8.5 and 4.5.

Damage functions. We take the damage functions that indicate how changes in local winter temperature affect fundamental productivity and amenities, $\Lambda^a(\Delta T_t(r), T_{t-1}(r))$ and $\Lambda^b(\Delta T_t(r), T_{t-1}(r))$, from Cruz and Rossi-Hansberg (2024). Figure A1 displays their estimates.

Figure A1: Damage Functions of Amenities and Productivity

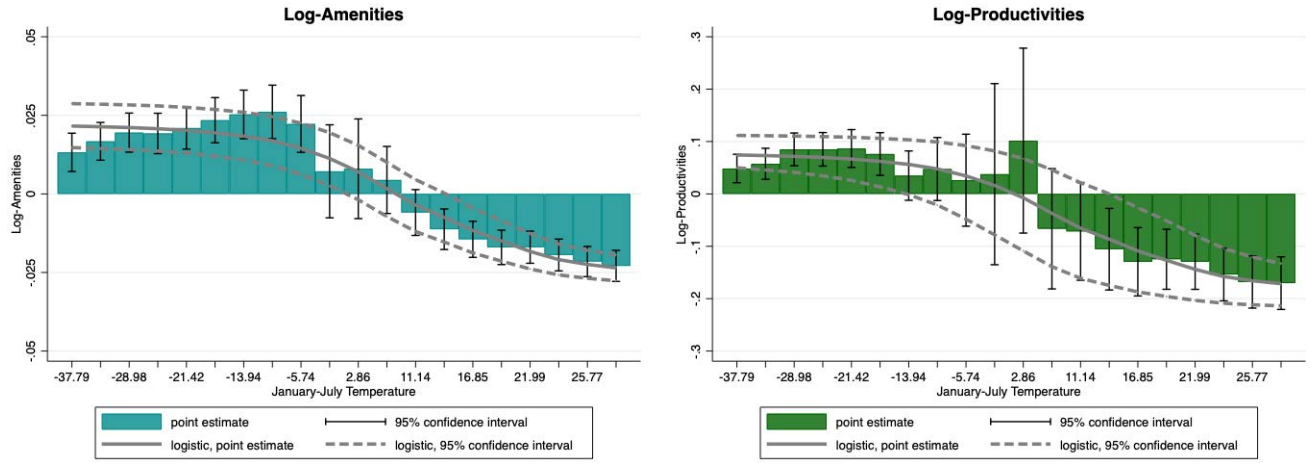

(a) Amenities (b) Productivity

Source: Cruz and Rossi-Hansberg (2024).

B Additional Figures

Figure B.1: Welfare Impact of Global Warming Without an AMOC Collapse (Restricted Welfare Range)

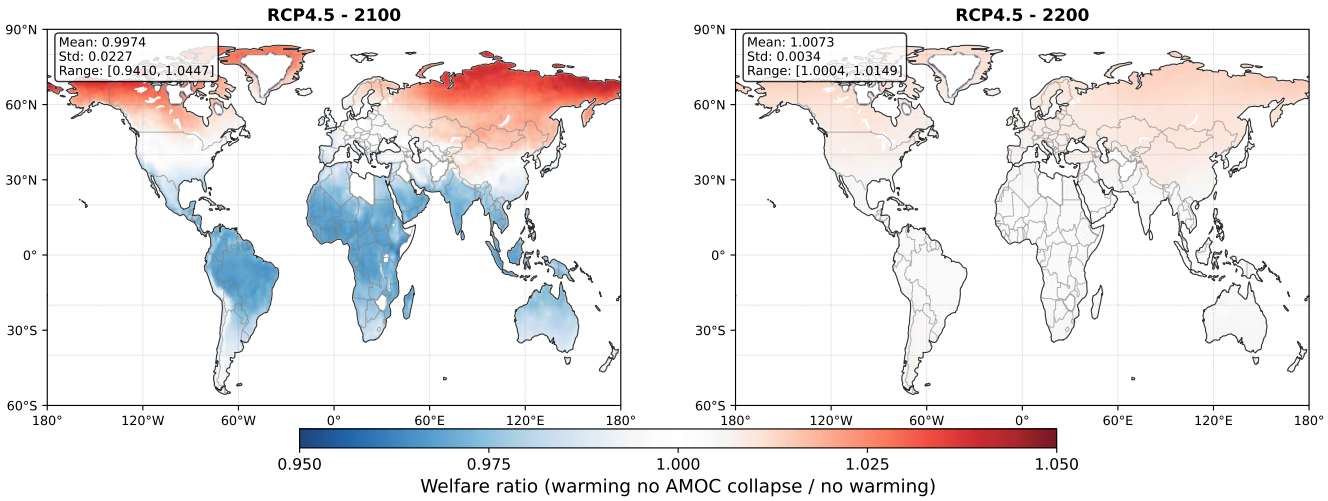

This figure shows welfare in a world with global warming and no AMOC collapse relative to welfare in a world without further global warming post 2022 for RCP4.5 in 2100 (panel (a)) and 2200 (panel (b)). It reproduces Figure 4 but restricts the welfare ratio from 0.95 to 1.05 to make smaller changes visible. The mean reported in the top left corner of each map is the unweighted average across grid cells.

Figure B.2: Effects of an AMOC Collapse Without Migratory Response (Restricted GDP Range)

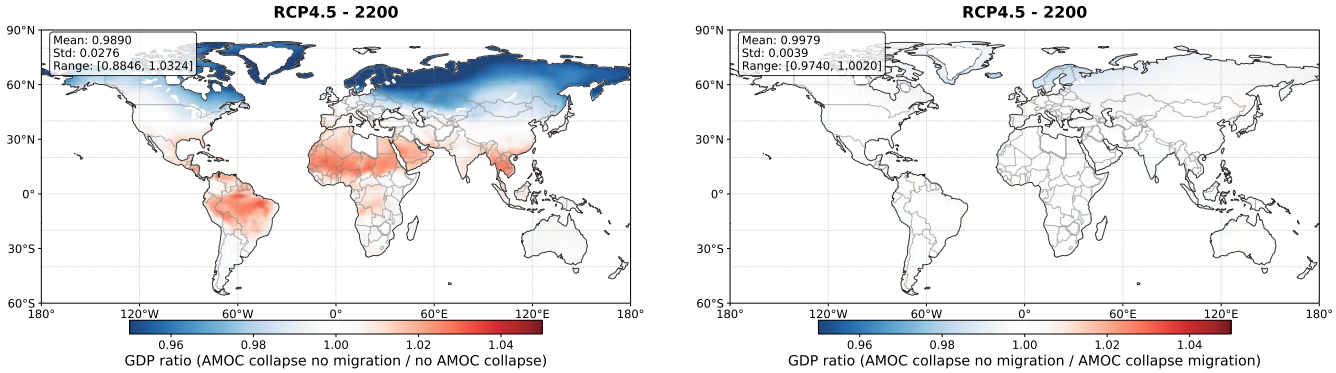

(a) GDP p.c. relative to no AMOC collapse

(b) GDP p.c. relative to AMOC collapse with migration

Panel (a) shows for the year 2200 and under RCP4.5 the ratio of real GDP per capita in an economy with an AMOC collapse but no migratory response to the collapse relative to an economy with no AMOC collapse (panel (a)), and relative to an economy with an AMOC collapse and the possibility to respond to the collapse by migrating (panel (b)). It reproduces panels (c) and (d) of Figure 12 but restricts real GDP per capita ratio from 0.95 to 1.05 to make smaller changes visible. The mean reported in the top left corner of each map is the unweighted average across grid cells.

Figure B.3: Effects of an AMOC Collapse Without Migratory Response (RCP8.5)

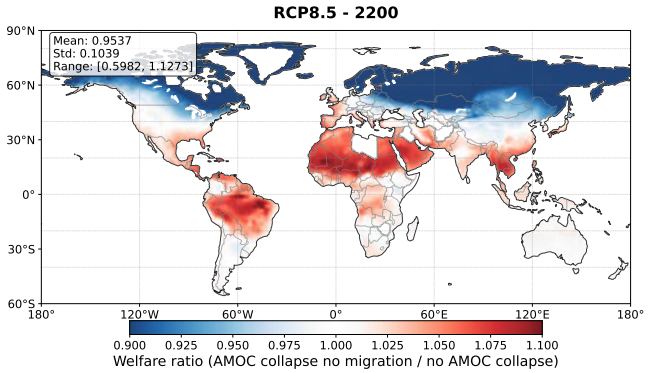

(a) Welfare relative to no AMOC collapse

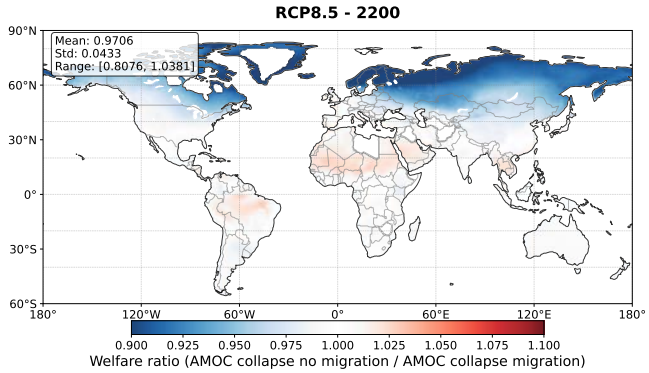

(b) Welfare relative to AMOC collapse with migration

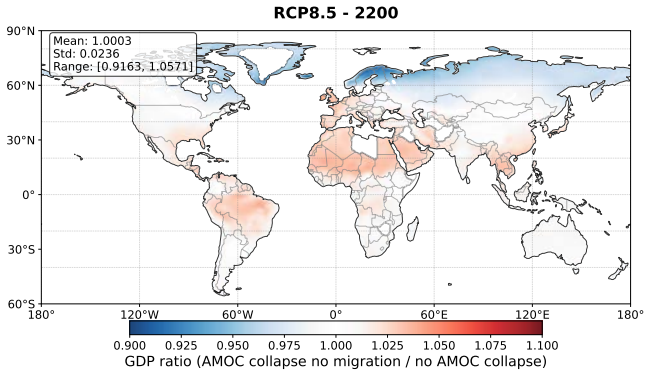

(c) GDP p.c. relative to no AMOC collapse

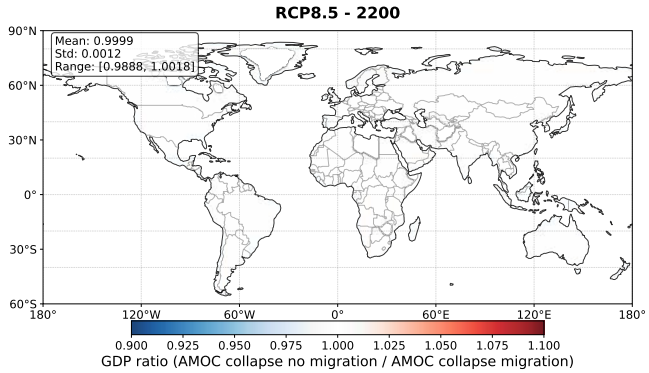

(d) GDP p.c. relative to AMOC collapse with migration

Panel (a) shows for the year 2200 and under RCP8.5 the ratio of welfare in an economy with an AMOC collapse but no migratory response to the collapse relative to an economy with no AMOC collapse (panel (a)), and relative to an economy with an AMOC collapse and the possibility to respond to the collapse by migrating (panel (b)). Panels (c) and (d) show the corresponding ratios for real GDP per capita. The mean reported in the top left corner of each map is the unweighted average across grid cells.